TABLE II. Patients Characteristics

Therapy groups	G1	G2	G3	G4	Total (%)
No. of patients	17	103	111	90	321
Sex					
Male	12	72	90	71	245 (76)
Female	5	31	21	19	76 (24)
Age					
0–4	2	12	18	16	48 (15)
5–9	3	45	42	39	129 (40)
10–14	8	42	42	27	119 (37)
15–	4	4	9	8	25 (8)
Histology					
BL/BLL/B-ALL	5	33	62	80	180 (56)
DLBCL	12	58	26	5	101 (31.4)
MLBCL	0	0	2	0	2 (0.6)
Others	0	12	21	5	38 (12)
Primary sites					
Thorax	5	30	7	1	43
Head & neck	5	39	12	2	58
Peripheral lymph nodes	0	3	3	0	6
Abdomen	7	29	75	11	122
Mediastinum	0	0	8	0	8
B-ALL	0	0	0	73	73
CNS	0	0	0	2	2
Other tumor site	0	2	5	0	7
Not specified	0	0	1	1	2
BM involvement	0	0	22	80	102 (32)
CNS involvement	0	0	0	38	38 (12)

BL, Burkitt lymphoma; BLL, Burkitt-like lymphoma; B-ALL, Burkitt leukemia; DLBCL, diffuse large B-cell lymphoma, MLBCL, mediastinal large.

for patients (n = 10) with CNS involvement only (BM−, CNS+), and 75.0% ± 8.2% for patients (n = 28) with BM and CNS involvements (BM+/CNS+), ($P = 0.102$) (Fig. 3D). Outcome by treatment response to initial A courses were as follows: The 4-year OS and EFS for patients who achieved CR (n = 236) or CRu (n = 54) at the last evaluation time were 95.7% ± 1.6% and 93.5% ± 1.6%, and 96.1% ± 2.7% and 86.9% ± 4.6%, respectively, while the 4-year OS and EFS for patients (n = 13) who did not achieve CR/CRu was 69.2% ± 12.8% and 15.4% ± 10.1% ($P < 0.001$), respectively.

Treatment Failure Events

Forty patients experienced an event and 25 have died (Fig. 2). The cause of death was tumor progression in 14, infection in 7, stem cell transplantation-related death in 3, and pulmonary bleeding in 1. The 40 events consisted of 13 induction failures, 6 deaths, 20 relapses, and one second cancer. Of the13 patients (6 in Group 3 and 7 in Group 4) who failed the initial treatment, 4 patients in Group 3 received salvage therapy and achieved CRu. At the time of the last analysis, 8 patients (4 in Group 3 and 4 in Group 4) were alive without tumor. Death in remission occurred in 3/321 (1%) patients: two died of infection and one died of pulmonary bleeding. The longest duration before relapse from the start of therapy was 38.9 months in DLBCL and 13.6 months in Burkitt histology. Relapse sites were 10 in local, 6 in BM, 2 in BM+CNS, one in local + CNS, and one in CNS. All CNS relapse occurred in patients with BL, but not with DLBCL. Thus, isolated CNS failure was only one among 38 patients with CNS involvement. Of the 20 relapsed patients, 11 died and 9 survived without tumor. A second cancer occurred among the patients who failed the initial treatment: a 12-year-old male with BL developed a secondary malignancy with acute myeloid leukemia (FAB M5) 17 months after the initial diagnosis.

Toxicity

Acute toxicity of treatment courses (A and B) was evaluated by the scale of NCI-CTC version 2.0., and rates of acute toxicity Grade 3 among patients in Groups 2, 3, and 4 are shown in Supplemental Table I. Anemia and neutropenia were the most frequent hematological toxicities with grade III or IV in all groups. In particular, grade IV neutropenia occurred in almost all patients (>98%) during A courses. In nonhematologic toxicity, infection was the single most frequent occurring with grade III or IV at least once in 70% of patients although the rate of grade IV infection was very small (<1%). Stomatitis and hepatotoxicity were also frequent, occurring with grade III or IV at least once in 20–35% and 24–38% of patients, respectively. The rate of renal toxicity grade III was very low. Leukoencephalopathy was reported in two patients of Group 3, and their MRI findings disappeared within 2 months without neurological symptoms. The overall incidence of renal insufficiency associated with tumor lysis syndrome was 2 out of 96 (2%) in Group 4, and these required assisted renal support with continuous hemodiafiltration.

DISCUSSION

During the last two decades, the survival outcome of children with B-NHL has been markedly improved through consecutive

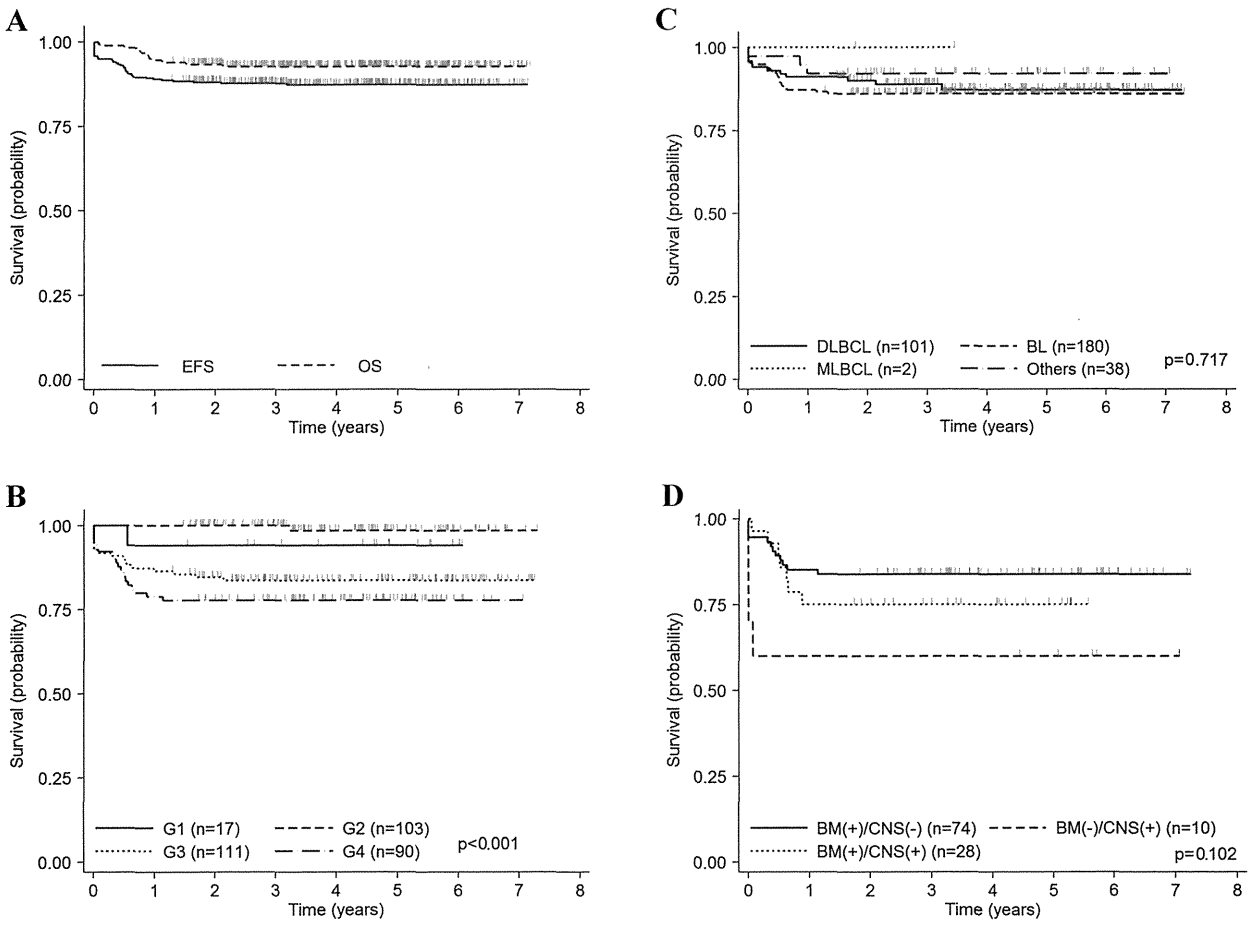

Fig. 3. Kaplan–Meier curves for OS and EFS of all patients (**A**). Kaplan–Meier curves for EFS according to treatment group (**B**), histology (**C**), and BM/CNS involvement (**D**).

clinical trials in large study groups, and the cure rate of childhood B-NHL has reached 90% [1–6]. In the present study, we showed an excellent survival outcome with 4-year OS 93% in children with B-NHL. In our study, the 4-year EFS 84% of Group 3 patients was considerably lower than the 4-year EFS 90% of intermediate risk group in the FAB/LMB96 study [5] or the 6-year EFS 88% of stage III patients in the BFM90 study [2], whereas, the 4-year EFS 78% of Group 4 patients compared favorably with the 4-year EFS 79% of high-risk group in the FAB/LMB96 study [5] and the 6-year EFS 74% of stage IV/B-ALL patients in the BFM90 study [2]. This outcome was obtained via the short-intensive chemotherapy regimen based on COPAD (CPM, VCR, PSL, and ADR) regimen plus the HDMTX of the lymphomas malin B (LMB) studies [3]. We omitted cranial irradiation for all patients, because recent studies have suggested the possibility of deleting radiotherapy in treating CNS diseases as well as CNS prophylaxis [2,3,5,9]. However, having no experience in administrating 8 g/m^2 HDMTX, we employed 5 g/m^2 HDMTX over 24 hour-infusion and not the 8 g/m^2 HDMTX over 4 hour-infusion in the LMB protocols for treating patients with CNS disease [3,5]. The treatment result for CNS disease was satisfactory, because CNS failure was only one of 38 patients with primary CNS disease in the present study.

This suggests that the 5 g/m^2 HDMTX over 24 hour-infusion is equally as effective to the CNS-positive disease as the aforementioned 8 g/m^2 HDMTX over 4 hours infusion, and reinforces the possibility that CNS irradiation could be omitted without jeopardizing the outcome of patients with CNS disease by using systemic and it MTX therapy [3,5,9].

The treatment of DLBCL as well as BL was another important focus of our study, because the incidence of DLBCL in childhood B-NHL is relatively more frequent than that of Western countries: the number of DLBCL was almost similar to that of BL (excluding B-ALL) in the present study and our recent national survey for childhood hematological malignancies has shown that the ratio of DLBCL to BL was 0.79 [14]. In our study, according to the strategy that DLBCL was treated by short-pulse chemotherapy as well as BL [15], we followed the same protocol, and achieved a favorable outcome of 4-year EFS with 87% for DLBCL which was not inferior to that of BL. This outcome can be partly explained by shared biological features, that is, that more than half of childhood DLBCL has the molecular subtypes of BL [16].

Several factors associated with poor outcome in the high-risk group in childhood B-NHL have been reported. Cairo et al. has shown a significantly inferior outcome (4-year EFS 61% ± 6%) of the subgroup of children with combined BM and CNS involvement at diagnosis as compared with children with BM or CNS only [5]. However, our results in Group 4 showed that the outcome (4-year EFS 75% ± 8%) of this subgroup with BM+/CNS+ was not significantly inferior than that of the subgroup with BM+ (83% ± 4%) or CNS+ (60% ± 1%). Failure to initial therapy is

also known to be a strong, unfavorable prognostic factor. Past studies in LMB 89/96 have shown that non-responders to pre-phase therapy (COP regimen) suffer a significantly inferior outcome as compared with responders or incomplete responders [3,5]. In our study, an appropriate evaluation of tumor regression just after pre-phase therapy was difficult for many patients, such that we compared the outcome according to response at the final evaluation time after two or three courses of therapy. These results showed that 4-year EFS of patients who did not achieve CR/CRu was only $15\% \pm 10\%$, which was as dismal as the outcome of poor-responders to COP regimen in the FAB/LMB 96 study [5]. To rescue the poor-responders in our study, we employed salvage therapy with high-dose Ara-C and VP16 to patients who did not achieve remission after 2 or 3 courses of therapy in Group 2 or 3, as in the BFM90 or FAB96 study [2,4]. As a result, 4 of 6 patients in Group 3 received salvage therapy and survived without tumor. This response rate was similar to that of FAB96 study, in which 10 out of 16 patients who received the second phase treatment intensification after the consolidation phase were alive. Thus, our results reconfirmed the efficacy of the salvage therapy.

Management of acute toxicity by short-pulse intensive chemotherapy is essential to successfully carry out the treatment protocol for childhood B-NHL. In our study, grade IV neutropenia occurred in almost all patients, but the rate of grade IV infection was quite low. Consequently, therapy-related death was less than 1% in all patients, and 2.1% in Group 4 patients. These results show the safety and feasibility of our treatment protocol. Anthracycline cardiotoxicity and secondary malignancy by alkylating agents are serious late events in pediatric cancer treatment [17,18]. To reduce the risk of cardiotoxicity, we employed THP-adriamycin (pirarubicin) instead of ADR. Pirarubicin is a derivative of ADR with reportedly less cardiotoxicity in adults [19–24]. Recently, we have reported that no significant cardiac dysfunction was detected in long-term survivors of children with acute lymphoblastic leukemia who received THP treatment [25–27]. In the present study, there were no patients with cardiac insufficiency or cardiac myopathy during the 7-year observation period. These results suggest that late-onset cardiotoxicity induced by pirarubicin is uncommon in childhood lymphoid malignancies, at least up to the cumulative dose of 240 mg/m^2. In our study, there was one male with a second cancer with acute myeloid leukemia, although the correlation between his second cancer and the protocol treatment is uncertain because he was resistant to the pre-phase followed by arbitrary treatment.

As shown above, chemotherapy-related toxicity of our protocol treatment was within acceptable range. However, a 6-course treatment for Group 3 seemed to be more intensive as compared with a 4-course treatment for intermediate risk group in the FAB96 study [4]. In order to reduce the total dose of cytotoxic drugs without impairing the survival outcome, new approaches including targeted monoclonal antibody therapy in combination with chemotherapy [28,29], are needed for children with an advanced or resistant disease in coming studies.

In conclusion, our nationwide study resulted in a cure rate above 90% with <1% toxic death in childhood B-NHL.

ACKNOWLEDGMENTS

We would like to thank all of the patients who enrolled in the B-NHL03 study and their families. This study was supported by Grants for Clinical Cancer Research from the Ministry of Health, Labor and Welfare of Japan; H14-Koka(Gan)-031, H15-Koka(Gan)-024, H16-GanRinsho-004, H17-GanRinsho-004, H20-GanRinsho-Ippan-017, H23-GanRinsho-Ippan-014.

REFERENCES

1. Reiter A, Schrappe M, Parwaresch R, et al. Non-Hodgkin's lymphomas of childhood and adolescence: Results of a treatment stratified for biologic subtypes and stage. A report of the Berlin Frankfurt-Münster Group. J Clin Oncol 1995;13:359–372.
2. Reiter A, Schrappe M, Tiemann M, et al. Improved treatment results in childhood B-cell neoplasms with tailored intensification of therapy: Reports of the Berlin–Frankfurt–Münster Group trial NHL–BFM 90. Blood 1999;94:3294–3306.
3. Patte C, Auperin A, Michon J, et al. The Société Française d'Oncologie Pédiatrique LMB89 protocol: Highly effective multiagent chemotherapy tailored to the tumor burden and response in 561 unselected children with B-cell lymphomas and L3 leukemia. Blood 2001;97:3370–3379.
4. Patte C, Auperin A, Gerrard M, et al. Results of the randomized international FAB/LMB96 trial for intermediate risk B-cell non-Hodgkin lymphoma in children and adolescents. It is possible to reduce treatment for the early responding patients. Blood 2007;109:2773–2780.
5. Cairo MS, Gerrard M, Sposto R, et al. Results of a randomized international study of high-risk central nervous system B non-Hodgkin lymphoma and B acute lymphoblastic leukemia in children and adolescents. Blood 2007;109:2736–2743.
6. Gerrard M, Cairo MS, Weston C, et al. Excellent survival following two courses of COPAD chemotherapy in children and adolescents with resected localized B-cell non-Hodgkin's lymphoma: Results of the FAB/LMB 96 international study. Br J Haematol 2008;141:840–847.
7. Shimizu H, Kikuchi M, Takaue Y, et al. Improved treatment results of non-Hodgkin's lymphoma in children: A report from the Children's Cancer and Leukemia Study Group of Japan. Int J Hematol 1995;61:85–96.
8. Horibe K, Akiyama Y, Kobayashi M, et al. Treatment outcome of AT-B88 regimen for B-cell non-Hodgkin's lymphoma and surface immunoglobulin-positive acute lymphoblastic leukemia in children. Int J Hematol 1997;66:89–98.
9. Tsurusawa M, Taga T, Horikoshi Y, et al. Favourable outcomes in children with diffuse large B-cell lymphoma treated by a short-term ALL-like regimen: A report on the NHL960 study from the Japanese Childhood Cancer and Leukemia Study Group. Leuk Lymphoma 2008;49:734–739.
10. Kikuchi A, Mori T, Fujimoto J, et al. Outcome of childhood B-cell non-Hodgkin lymphoma and B-cell acute lymphoblastic leukemia treated with the Tokyo Children's Cancer Study Group NHL B9604 protocol. Leuk Lymphoma 2008;49:757–762.
11. Lee SH, Yoo KH, Sung KW, et al. Should children with non-Hodgkin lymphoma be treated with different protocols according to histopathologic subtype? Pediatr Blood Cancer 2013;60:1842–1847.
12. Jaffe ES, Harris NL, Stein H, et al., editors. WHO classification of tumors, pathology and genetics of tumors of haematopoietic and lymphoid tissues. Lyon: IARC Press; 2001.
13. Murphy SB. Classification, staging and results of treatment of childhood NHL, dissimilarities from lymphoma in adults. Seminars in Oncology 1980;7:332–339.
14. Horibe K, Saito AM, Takimoto T, et al. Incidence and survival rates of hematological malignancies in Japanese children and adolescents (2006-2010): Based on registry data from the Japanese Society of Pediatric Hematology. Int J hematol 2013;98:74–88.
15. Reiter A, Klapper W. Recent advances in the understanding and management of diffuse large B-cell lymphoma in children. Br J Haematol 2008;142:329–347.
16. Klapper W, Szczepanowski M, Burkhardt B, et al. Molecular profiling of pediatric mature B-cell lymphoma treated in population-based prospective clinical trials. Blood 2008;112:1374–1381.
17. Sorensen K, Levitt GA, Bull C, et al. Late anthracycline cardiotoxicity after childhood cancer: A prospective longitudinal study. Cancer 2003;97:1991–1998.
18. Davies SM. Subsequent malignant neoplasms in survivors of childhood cancer: Childhood Cancer Survivor Study (CCSS) studies. Pediatric Blood Cancer 2007;48:727–730.
19. Umezawa H, Takahashi Y, Kinoshita M, et al. Tetrahydropyranyl derivatives of daunomycin and adriamycin. J Antibiot 1979;32:1082–1084.
20. Takagi T, Sakai C, Oguro M. Combination chemotherapy with pirarubicin (THP), cyclophosphamide, vincristine, and prednisolone (VEP-THP therapy) in the treatment of non-Hodgkins lymphoma. Oncology 1990;47:25–28.
21. Niitsu N, Umeda M. Biweekly THP-COPBLM (pirarubicin, cyclophosphamide, vincristine, prednisone, bleomycin and procarbazine) regimen combined with granulocyte colony-stimulating factor (G-CSF) for intermediate- and high-grade non-Hodgkins's lymphoma. Leukemia 1998;12:1457–1460.
22. Niitsu N, Umeda M. Response and adverse drug reactions to combination chemotherapy in elderly patients with aggressive non-Hodgkin's lymphoma: Comparison of CHOP, COP-BLAM, COP-BLAM III, and THP-COPBLM. Eur J Haematol 1999;63:337–344.
23. Tsurumi H, Yamada T, Sawada M, et al. Biweekly CHOP or THP-COP regimens in the treatment of newly diagnosed aggressive non-Hodgkin's lymphoma. A comparison of doxorubicin and pirarubicin: A randomized phase II study. J Cancer Res Clin Oncol 2004;130:107–113.
24. Zhai L, Guo C, Cao Y, et al. Long-term results of pirarubicin versus doxorubicin in combination chemotherapy for aggressive non-Hodgkin's lymphoma: Single center, 15-year experience. Int J Hematol 2010;91:78–86.
25. Tsurusawa M, Shimomura Y, Asami K, et al. Long-term results of the Japanese Childhood Cancer and Leukemia Study Group studies 811, 874 and 911 on childhood acute lymphoblastic leukemia. Leukemia 2010;24:335–344.
26. Yamaji K, Okamoto T, Yokota S, et al. Minimal residual disease-based augmented therapy in childhood acute lymphoblastic leukemia: A report from the Japanese Childhood Cancer and Leukemia Study Group Study. Pediatr Blood Cancer 2010;55:1287–1295.
27. Shimomura Y, Baba R, Watanabe A, et al. Japanese Childhood Cancer and Leukemia Study Group (JCCLSG). Assessment of late cardiotoxicity of pirarubicin (THP) in children with acute lymphoblastic leukemia. Pediatr Blood Cancer 2011;57:461–466.
28. Meinhardt A, Burkhardt B, Zimmermann M, et al. Phase II window study on rituximab in newly diagnosed pediatric mature B-cell non-Hodgkin's lymphoma and Burkitt leukemia. J Clin Oncol 2010;28:3115–3121.
29. Barth MJ, Goldman S, Smith L, et al. Rituximab pharmacokinetics in children and adolescents with de novo intermediate and advanced mature B-cell lymphoma/leukaemia: A Children's Oncology Group report. Br J Haematol 2013;162:678–683.

ORIGINAL ARTICLE

Hepatocytes Buried in the Cirrhotic Livers of Patients With Biliary Atresia Proliferate and Function in the Livers of Urokinase-Type Plasminogen Activator–NOG Mice

Hiroshi Suemizu,[1]* Kazuaki Nakamura,[3]* Kenji Kawai,[2] Yuichiro Higuchi,[1] Mureo Kasahara,[4] Junichiro Fujimoto,[5] Akito Tanoue,[3] and Masato Nakamura[6]

[1]Biomedical Research Department, and [2]Pathology Research Department, Central Institute for Experimental Animals, Kanagawa, Japan; [3]Department of Pharmacology, [4]Department of Transplant Surgery, and [5]Clinical Research Center, National Center for Child Health and Development, Tokyo, Japan; and [6]Department of Pathology and Regenerative Medicine, Tokai University School of Medicine, Kanagawa, Japan

The pathogenesis of biliary atresia (BA), which leads to end-stage cirrhosis in most patients, has been thought to inflame and obstruct the intrahepatic and extrahepatic bile ducts. BA is not believed to be caused by abnormalities in parenchymal hepatocytes. However, there has been no report of a detailed analysis of hepatocytes buried in the cirrhotic livers of patients with BA. Therefore, we evaluated the proliferative potential of these hepatocytes in immunodeficient, liver-injured mice [the urokinase-type plasminogen activator (uPA) transgenic NOD/Shi-scid IL2rγnull (NOG); uPA-NOG strain]. We succeeded in isolating viable hepatocytes from the livers of patients with BA who had various degrees of fibrosis. The isolated hepatocytes were intrasplenically transplanted into the livers of uPA-NOG mice. The hepatocytes of only 3 of the 9 BA patients secreted detectable amounts of human albumin in sera when they were transplanted into mice. However, human leukocyte antigen–positive hepatocyte colonies were detected in 7 of the 9 mice with hepatocyte transplants from patients with BA. We demonstrated that hepatocytes buried in the cirrhotic livers of patients with BA retained their proliferative potential. A liver that was reconstituted with hepatocytes from patients with BA was shown to be a functioning human liver

Additional Supporting Information may be found in the online version of this article.

Abbreviations: 5-CF, 5-carboxyfluorescein; 5-CFDA, 5(6)-carboxyfluorescein diacetate; αSMA, alpha smooth muscle actin; ABC, adenosine triphosphate–binding cassette; ALB, albumin; BA, biliary atresia; BC, bile canaliculus; CFDA, 5-carboxyfluorescein diacetate; CYP, cytochrome P450; GAPDH, glyceraldehyde-3-phosphate dehydrogenase; hALB, human albumin; H&E, hematoxylin and eosin; HIF, high intrinsic fluorescence; HLA, human leukocyte antigen; IF, intrinsic fluorescence; LT, liver transplantation; MRP2, multidrug resistance–associated protein 2; ND, not detected by an enzyme-linked immunosorbent assay; NGS, normal goat serum; NMS, normal mouse serum; NR1, nuclear receptor subfamily 1; NRS, normal rabbit serum; PELD, Pediatric End-Stage Liver Disease; PI, propidium iodide; SLC, solute carrier family; UGT, uridine diphosphate glucuronosyltransferase; uPA, urokinase-type plasminogen activator; VIM, vimentin.

The authors report no conflicts of interest.

Hiroshi Suemizu was the primary experimenter, performed all transplants, analyzed the liver-reconstituted mice, and wrote the article. Kazuaki Nakamura, Mureo Kasahara, Junichiro Fujimoto, and Akito Tanoue performed all isolations of human hepatocytes and managed all the clinical samples. Kenji Kawai provided all the tissue histology. Yuichiro Higuchi analyzed the liver-reconstituted mice. Masato Nakamura provided overall project planning and coordination.

This work was supported in part by Grants-in-Aid for Scientific Research to Hiroshi Suemizu (21240042) and Akito Tanoue (23300162) from the Japan Science and Technology Agency.

*These authors contributed equally to this work.

Address reprint requests to Hiroshi Suemizu, Ph.D., Biomedical Research Department, Central Institute for Experimental Animals, 3-25-12 Tonomachi, Kawasaki-Ku, Kawasaki, Kanagawa 210-0821, Japan. Telephone: +81-44-201-8530; FAX: +81-44-201-8541 or +81-44-201-8511; E-mail: suemizu@ciea.or.jp or nogmouse@ciea.or.jp

DOI 10.1002/lt.23916
View this article online at wileyonlinelibrary.com.
LIVER TRANSPLANTATION.DOI 10.1002/lt. *Published on behalf of the American Association for the Study of Liver Diseases*

with a drug-metabolizing enzyme gene expression pattern that was representative of mature human liver and biliary function, as ascertained by fluorescent dye excretion into the bile canaliculi. These results imply that removing the primary etiology via an earlier portoenterostomy may increase the quantity of functionally intact hepatocytes remaining in a cirrhotic liver and may contribute to improved outcomes. *Liver Transpl 20:1127-1137, 2014.* © 2014 AASLD.

Received January 2, 2014; accepted May 10, 2014.

Biliary atresia (BA), the most common pediatric cholestatic disease, is caused by the progressive fibro-obliterative obstruction of the extrahepatic and intrahepatic bile ducts within the first few weeks of life.[1,2] The current surgical treatment is sequential. In the first few weeks of life, a Kasai portoenterostomy is performed to bypass the obstructed extrahepatic bile ducts and restore the biliary flow.[3] Approximately 20% of all patients who undergo portoenterostomy during infancy survive into adulthood with their native liver.[2,4] In general, it is advantageous to perform portoenterostomy as early after birth as possible to optimize the chance of success.[5] Patients who fail to undergo portoenterostomy experience a gradual deterioration of liver function and develop progressive fibrosclerosis; after the initial successful establishment of bile flow, liver transplantation (LT) is the only treatment option. Although several etiologies of BA have been postulated, the precise pathogenesis of BA remains unknown. Some factors that might contribute to its development are genetic, infective, inflammatory, and toxic insults.[1] In most cases, BA is associated with an intensive inflammatory infiltrate; this knowledge led us to the conjecture that BA results from an infectious or autoimmune destruction of the bile ducts. For example, the infection of newborn mice with the Rhesus rotavirus results in a BA-like disease.[6-8] Meanwhile, hepatocytes from patients with BA have not been thought to be involved in the development of chronic obstructive cholestasis. We and other groups have developed mice with humanized livers in which the liver is reconstituted with human hepatocytes so that in vivo drug metabolism and liver regeneration can be studied.[9-11] Therefore, the aims of this study were to evaluate the in vivo proliferative potential and functional properties of hepatocytes buried in the cirrhotic livers of BA patients.

MATERIALS AND METHODS

Specimens from the National Research Institute for Child Health and Development were collected in a standardized manner with the permission of the patients' families.

Animals

All mouse studies were conducted in strict accordance with *Guide for the Care and Use of Laboratory Animals* from the Central Institute for Experimental Animals. All experimental protocols were approved by the animal care committee of the Central Institute for Experimental Animals (permit number 11029A). All surgeries were performed under isoflurane anesthesia, and all efforts were made to minimize animal suffering. All studies using mouse tissue with transplanted human cells were approved by the ethics and biosafety committee of the National Research Institute for Child Health and Development and the Central Institute for Experimental Animals. The urokinase-type plasminogen activator (uPA) transgenic NOD/Shi-scid IL2rγnull (NOG); uPA-NOG strain[11] was maintained through the breeding of a female uPA-NOG hemizygote with a male homozygote. The zygosity of the *uPA* transgene was presumed from the degree of liver damage, which was examined through the determination of the serum levels of alanine aminotransferase with a Fuji DRI-CHEM 7000 clinical biochemical analyzer (Fujifilm Corp., Tokyo, Japan). The uPA-NOG mice with serum alanine aminotransferase activity greater than 150 U/L were selected as homozygotes and were then used as transplant recipients.

Isolation of Hepatocytes From the Livers of Patients With BA

The entire experimental protocol was approved by the ethics and research committee of the National Center for Child Health and Development. Written informed consent was obtained in each case. Except for the pieces of liver tissue that were used as pathological specimens, the enucleated diseased livers from the transplant recipients were discarded. The human hepatocytes used in this study were procured from liver tissue removed from BA patients who met the diagnostic criteria [Pediatric End-Stage Liver Disease (PELD) score[12] $\geq$ 6 points] for LT operations. The levels of fibrosis were categorized according to the following criteria: (I) mild (portal fibrous expansion to bridging fibrosis involving $\leq$50% of portal tracts), (II) moderate (bridging fibrosis involving >50% of portal tracts), and (III) severe (bridging fibrosis involving >50% of the portal tracts with nodular architectural changes).[13] Patient 141, who had grade III fibrosis and a PELD score of 0, had portopulmonary syndrome (intrapulmonary shunting). The shunt ratio, calculated with technetium-99m macroaggregated albumin (ALB) scintigraphy, was 16.8%, which indicated a relatively mild shunt. The hepatocytes were isolated from the resected liver tissue through the 2-step collagenase perfusion[14] of the liver samples, as described previously.[15] Hepatic parenchymal cells were isolated with low-speed centrifugation (50*g*). Cell numbers and viability were assessed with trypan blue exclusion.[16]

Flow Cytometry Analysis

The hepatocytes were stained with 1 mg/mL propidium iodide (PI; Sigma-Aldrich Co. LLC, St. Louis, MO), which stains dead cells. The intensity of 502-nm fluorescence was measured as intrinsic fluorescence (IF). Flow cytometry data were collected with a FACSCanto analyzer and BD FACSDiva software (BD Biosciences, Franklin Lakes, NJ). The data were analyzed with the FlowJo program (Tree Star, Inc., Ashland, OR).

Transplantation of Hepatocytes Into uPA-NOG Mice

Hepatocytes from patients with BA and commercially available cryopreserved human hepatocytes from a 4-year-old female (NHEPS, Lonza, Walkersville, MD) were used as donor cells. Young (8-week-old) male uPA-NOG mice were used as the recipients of the human hepatocytes. One million viable hepatocytes were injected intrasplenically via a Hamilton syringe with a 26-G needle. The successful engraftment of the human hepatocytes was evaluated through the measurement of the blood level of human albumin (hALB) with an hALB enzyme-linked immunosorbent assay quantitation kit (Bethyl Laboratories, Montgomery, TX) according to the manufacturer's protocol. The replacement index, which was the percentage of human donor hepatocytes in the recipient liver, was estimated according to the hALB concentration in chimeric mice.[17]

Histology and Immunohistochemistry

The tissues were fixed with 4% (vol/vol) phosphate-buffered formalin (Mildform, Wako Pure Chemical Industries, Ltd., Osaka, Japan), and 5-μm paraffin-embedded sections were stained with Azan-Mallory staining reagents (Muto Pure Chemicals, Tokyo, Japan) to visualize the collagen and muscle fibers and with hematoxylin and eosin (H&E). Some sections were autoclaved for 10 minutes in a target retrieval solution [0.1 M citrate buffer (pH 6.0) and 1 mM ethylene diamine tetraacetic acid (pH 9.0)] and were then equilibrated at room temperature for 20 minutes. Monoclonal mouse anti–human leukocyte antigen (anti-HLA) class I (A-C) antibodies (clone EMR8-5, Hokudo, Sapporo, Japan; 1:2000),[18] polyclonal goat anti-human ALB antibodies (Bethyl Laboratories; 1:1500), polyclonal rabbit anti-cytochrome P450 3A4 (CYP3A4) antibodies (Abcam, Inc., Cambridge, MA; 1:500), monoclonal mouse anti-human Ki-67 antigen antibodies (clone MIB-1; Dako Denmark A/S; 1:50),[19] monoclonal mouse anti-human multidrug resistance–associated protein 2 (MRP2) antibodies (clone M2 III-6, Millipore, Billerica, MA; 1:100),[20] monoclonal rabbit anti-vimentin (anti-VIM) antibodies (clone SP20, Nichirei Bioscience, Tokyo, Japan; 1:1500),[21] and monoclonal rabbit anti–alpha smooth muscle actin (anti-αSMA) antibodies (clone 1A4, Leica Microsystems, Tokyo, Japan; 1:200)[22] were used as primary antibodies. Normal mouse serum (NMS), normal goat serum (NGS), and normal rabbit serum (NRS) were used as negative controls for immunostaining. For bright-field immunohistochemistry, the antibodies for mouse, goat, and rabbit immunoglobulin were visualized with amino acid polymer/peroxidase complex–labeled antibodies [Histofine Simple Stain MAX PO (M, G, and R), Nichirei Bioscience) and a Bond Polymer Refine Detection system (Leica Microsystems) with a diaminobenzidine substrate [Dojindo Laboratories, Kumamoto, Japan; 0.2 mg/mL 3,3′-diaminobenzidine tetrahydrochloride, 0.05 M tris(hydroxymethyl)-aminomethane with hydrochloric acid (pH 7.6), and 0.005% hydrogen peroxide]. The sections were counterstained with hematoxylin. Hepatic biliary obstructions were examined with Hall's bilirubin staining method.[23] The images were captured under an Axio Imager upright microscope (Carl Zeiss, Thornwood, NY) equipped with AxioCam HRm and AxioCam MRc5 charge-coupled device cameras (Carl Zeiss).

Real-Time Quantitative Reverse-Transcription Polymerase Chain Reaction for Drug Metabolism–Related Gene Expression

The total cellular RNA was isolated from the livers with an RNeasy mini kit (Qiagen K.K.). Complementary DNA was synthesized with a high-capacity complementary DNA reverse transcription kit (Applied Biosystems, Foster City, CA) with random hexamers. TaqMan gene expression master mix and TaqMan gene expression assays (Applied Biosystems) were used for the real-time quantitative polymerase chain reactions; amplifications were performed with an ABI-Prism 7000 sequence detection system (Applied Biosystems). The comparative threshold cycle (Ct) method was used to determine the relative ratio of the gene expression for each gene, which was corrected with human glyceraldehyde-3-phosphate dehydrogenase (GAPDH) and referenced to the RNA extracted from donor hepatocytes. The TaqMan assay numbers are listed in Table 1.

Biliary Excretion Test With 5(6)-Carboxyfluorescein Diacetate (5-CFDA)

The ester precursor of 5-carboxyfluorescein (5-CF), 5(6)-carboxyfluorescein diacetate (5-CFDA; 0.5 nmol; Sigma-Aldrich), was injected intravenously into the mouse tail vein. Ten minutes after the 5-CFDA injection, the liver was perfused with 50 nmol/L 5-CFDA for 3 minutes, and the liver was then embedded in an optimum cutting temperature (O.C.T.) compound (Sakura Finetek Japan Co., Ltd., Tokyo, Japan) and frozen in liquid nitrogen. Ten-micrometer-thick serial frozen sections were prepared and air-dried. The 5-CF fluorescent signals were captured with an Axio Imager upright microscope (Carl Zeiss) equipped with AxioCam HRm and AxioCam MRc5 charge-coupled device cameras (Carl Zeiss). After the microfluorographs were taken, the tissue sections were fixed and rehydrated sequentially in decreasing concentrations of ethanol and water, and this was followed by immunohistochemical staining for MRP2. Sections were counterstained with

TABLE 1. TaqMan Probe Information

Gene Name	Gene Description	TaqMan Assay Number
GAPDH	Glyceraldehyde-3-phosphate dehydrogenase	Hs99999905_m1
ALB	Albumin	Hs99999922_s1
CYP1A1	Cytochrome P450, family 1, subfamily A, polypeptide 1	Hs00153120_m1
CYP1A2	Cytochrome P450, family 1, subfamily A, polypeptide 2	Hs00167927_m1
CYP2A6	Cytochrome P450, family 2, subfamily A, polypeptide 6	Hs00868409_s1
CYP2B6	Cytochrome P450, family 2, subfamily B, polypeptide 6	Hs03044634_m1
CYP2C8	Cytochrome P450, family 2, subfamily C, polypeptide 8	Hs00258314_m1
CYP2C9	Cytochrome P450, family 2, subfamily C, polypeptide 9	Hs00426397_m1
CYP2C18	Cytochrome P450, family 2, subfamily C, polypeptide 18	Hs00426400_m1
CYP2C19	Cytochrome P450, family 2, subfamily C, polypeptide 19	Hs00426380_m1
CYP2D6	Cytochrome P450, family 2, subfamily D, polypeptide 6	Hs00164385_m1
CYP2E1	Cytochrome P450, family 2, subfamily E, polypeptide 1	Hs00559368_m1
CYP3A4	Cytochrome P450, family 3, subfamily A, polypeptide 4	Hs00430021_m1
CYP3A5	Cytochrome P450, family 3, subfamily A, polypeptide 5	Hs00241417_m1
UGT1A1	Uridine diphosphate glucuronosyltransferase 1 family, polypeptide A1	Hs02511055_s1
UGT2B15	Uridine diphosphate glucuronosyltransferase 2 family, polypeptide B15	Hs00870076_s1
ABCB1	Adenosine triphosphate–binding cassette, subfamily B (MDR/TAP), member 1	Hs00184500_m1
ABCB11	Adenosine triphosphate–binding cassette, subfamily B (MDR/TAP), member 11	Hs00184824_m1
ABCC2	Adenosine triphosphate–binding cassette, subfamily C (CFTR/MRP), member 2	Hs00166123_m1
ABCG2	Adenosine triphosphate–binding cassette, subfamily G (WHITE), member 2	Hs01053790_m1
SLC22A1	Solute carrier family 22 (organic cation transporter), member 1	Hs00427552_m1
SLC22A7	Solute carrier family 22 (organic anion transporter), member 7	Hs00198527_m1
SLC22A9	Solute carrier family 22 (organic anion transporter), member 9	Hs00971064_m1
NR1H4	Nuclear receptor subfamily 1, group H, member 4	Hs00231968_m1
NR1I2	Nuclear receptor subfamily 1, group I, member 2	Hs00243666_m1
NR1I3	Nuclear receptor subfamily 1, group I, member 3	Hs00901571_m1

hematoxylin. Another tissue section was fixed in 4% paraformaldehyde, and this was followed by immunofluorescent staining with monoclonal mouse anti-HLA class I (A-C) antibodies, a streptavidin/Texas Red–labeled secondary antibody (GE Healthcare Bio-Sciences), and H&E. Commercially available cryopreserved human hepatocytes (normal hepatocytes) and cells from the HCT 116 line (American Type Culture Collection, Manassas, VA), a human colorectal carcinoma cell line that easily engrafts and forms tumor cell colonies in NOG mouse livers,[24] were used as positive and negative controls for the formulation of the bile canaliculus (BC) network.

Statistical Analyses

Group comparisons were performed with the Student *t* test for independent samples. *P* values less than 0.05 were considered significant (Prism 5, GraphPad Software, Inc., La Jolla, CA).

RESULTS

Engraftment of Hepatocytes From Patients With BA in uPA-NOG Mouse Livers

Using liver failure immunodeficient mouse models, we first evaluated the regenerative potential of the residual hepatocytes buried in the cirrhotic livers of patients with BA.[11] We succeeded in isolating viable hepatocytes from the livers of 9 BA patients with various degrees of fibrosclerosis (Table 2 and Fig. 1A). The typical gross morphology of a liver from a patient with BA is shown in Fig. 1B. There was no significant difference ($P = 0.45$) between the cell yields from patients with grade II fibrosis (2.3 ± 1.6 million cells per gram of liver, $n = 3$) and patients with grade III fibrosis (3.8 ± 4.2 million cells per gram of liver, $n = 6$; Fig. 1C). The cell viability was not significantly different ($P = 0.81$) between patients with grade II fibrosis ($76.7\% \pm 16.0\%$, $n = 3$) and patients with grade III fibrosis ($73.3\% \pm 23.0\%$, $n = 6$; Fig. 1D). The isolated hepatocytes were analyzed with flow cytometry (Fig. 1D). Because the IF signal of the hepatocytes from patients with BA was not increased in comparison with normal hepatocytes, it did not seem that bile accumulated within the hepatocytes, even in the patients with BA. The viable and engraftable hepatic parenchymal cells seemed to be present in the high intrinsic fluorescence (HIF) fraction; these cells had a very large cell mass and a complicated internal structure because the percentage of the HIF fraction correlated positively with the engraftability of the hepatocytes, which was based on the plasma concentration of hALB ($r^2 = 0.8784$; Fig. 1E, right). However, the cell viability did not show a direct correlation with the plasma concentration of hALB ($r^2 = 0.0515$; Fig. 1E, center) or the percentage of the HIF fraction ($r^2 = 0.0064$; Fig. 1E, left). The isolated hepatocytes were intrasplenically transplanted into uPA-NOG mice. Successful engraftment was evaluated in terms of the detection of hALB in the mouse serum

TABLE 2. Engraftment of Hepatocytes Derived From Patients With BA in uPA-NOG Mouse Livers

Patient Information							Experimental Condition and Summarized Results			
				Isolated Hepatocytes					Animals With Engraftment	
Number	Age	Sex	Fibrosis Level	PELD Score	Cells/g of Liver	Viability (%)	HIF (%)	Condition*	Cell Dose (Cells/Mouse)	HLA-Positive Colony [n/N (%)]†	hALB [n/N (μg/mL)]
80	10 months	Female	II	20	1.2×10^6	66	9.0	A	1.0×10^6	5/5 (100)	5/5 (230-875)
								B	1.0×10^6	4/4 (100)	1/4 (280)
								C	1.0×10^6	4/4 (100)	1/4 (38)
86	7 months	Female	II	35	1.5×10^6	95	4.8	A	1.0×10^6	2/2 (100)	1/2 (35)
								B	1.0×10^6	2/4 (50)	1/4 (105)
153	8 months	Male	II	9	4.1×10^6	69	1.3	B	1.0×10^6	2/3 (67)	0/3 (ND)
105	5 months	Female	III	13	1.2×10^7	83	8.5	B	1.0×10^6	4/4 (100)	4/4 (49-294)
133	6 months	Female	III	15	6.9×10^4	33	9.2	B	2.0×10^5	0/1 (0)	0/1 (ND)
141	12 years	Female	III	0	3.0×10^6	93	4.8	B	1.0×10^6	1/1 (100)	0/1 (ND)
149	8 months	Female	III	14	3.4×10^6	67	0.8	B	1.2×10^6	3/3 (100)	0/3 (ND)
151	5 months	Female	III	10	1.4×10^6	69	5.0	B	1.0×10^6	3/4 (75)	0/4 (ND)
154	6 months	Female	III	14	3.1×10^6	95	4.2	B	1.0×10^6	0/1 (0)	0/1 (ND)
77	32 years	Male	Normal	—	2.0×10^6	88	25.5	C	1.0×10^6	5/5 (100)	5/5 (35-516)

*The conditions were as follows: (A) fresh hepatocytes (within the first 6 hours after isolation), (B) chilled hepatocytes (stored at 4°C for more than 16 hours and up to 24 hours), and (C) cryopreserved hepatocytes.
†Hepatocyte colonies that contained more than 20 HLA-positive cells in the cross-sections.

and the appearance of HLA-positive hepatocyte colonies in the liver tissue (Fig. 1F). Although detectable amounts of secreted hALB were found only in the sera of mice that had received hepatocyte transplants from 3 of the 9 BA patients, HLA-positive hepatocyte colonies were detected as a result of 7 of the 9 hepatocyte transplants from patients with BA.

The expression of drug-metabolizing enzymes, a marker of a fully matured liver, was analyzed with real-time quantitative polymerase chain reaction. Livers reconstituted with hepatocytes from 2 different patients with BA (patients 80 and 105) and commercially available cryopreserved hepatocytes (NHEPS) were then examined. The relative gene expression profiles of hepatocytes from patients with BA were similar to those of NHEPS hepatocytes (Fig. 1G). The expression levels of most of the genes were higher in the reconstituted livers versus the donor hepatocytes (Fig. 1H).

Next, we examined the expression of ALB, a major functional marker of biosynthesis in the liver, via immunohistochemical staining with human-specific antibodies in hepatocytes originating from patients with BA (Fig. 2A, top and middle). This hepatic lineage marker protein was expressed within the human hepatocyte colonies in the reconstituted-liver mice at levels comparable to those of the liver reconstituted with cryopreserved normal hepatocytes (patient 77; Fig. 2A, bottom). The expression of CYP3A4, which is the main drug-metabolizing enzyme found in the liver, was also observed within the colonies consisting of both hepatocytes from patients with BA (Fig. 2A, top and middle) and normal hepatocytes (Fig. 2A, bottom), but it did not show the zonal distribution observed in the fully reconstituted uPA-NOG liver with NHEPS hepatocytes (Fig. 2B). Most human hepatocytes originating from the patients with BA were present as small foci that appeared to grow by clonal expansion within the uPA-NOG mouse livers. This growth was quite similar to that of normal hepatocytes from patient 77. In addition, immunohistochemical nuclear staining of serial sections of the mouse livers with an antibody (MIB-1) against the human Ki-67 antigen[25,26] revealed that the proliferative potential of the hepatocytes from the patients with BA was preserved, as evidenced by the nuclear staining of the hepatocytes located at the edges of human hepatocyte colonies (Fig. 2A, top and middle). NGS, NRS, and NMS (nonimmune), which corresponded to the host animals in which anti-ALB, anti-CYP3A4, and anti–Ki-67 antibodies, respectively, were prepared, did not react with either human or mouse hepatocytes (Fig. 2C). The hepatocyte colonies derived from the patients with BA were not stained by Azan-Mallory staining (Fig. 2A, top and middle).

Functional Integrity of Partially Humanized Livers

We confirmed the expression of MRP2 proteins on the plasma membranes of hepatocytes in both the livers of patients with BA and the partially humanized livers repopulated with hepatocytes from patients with BA

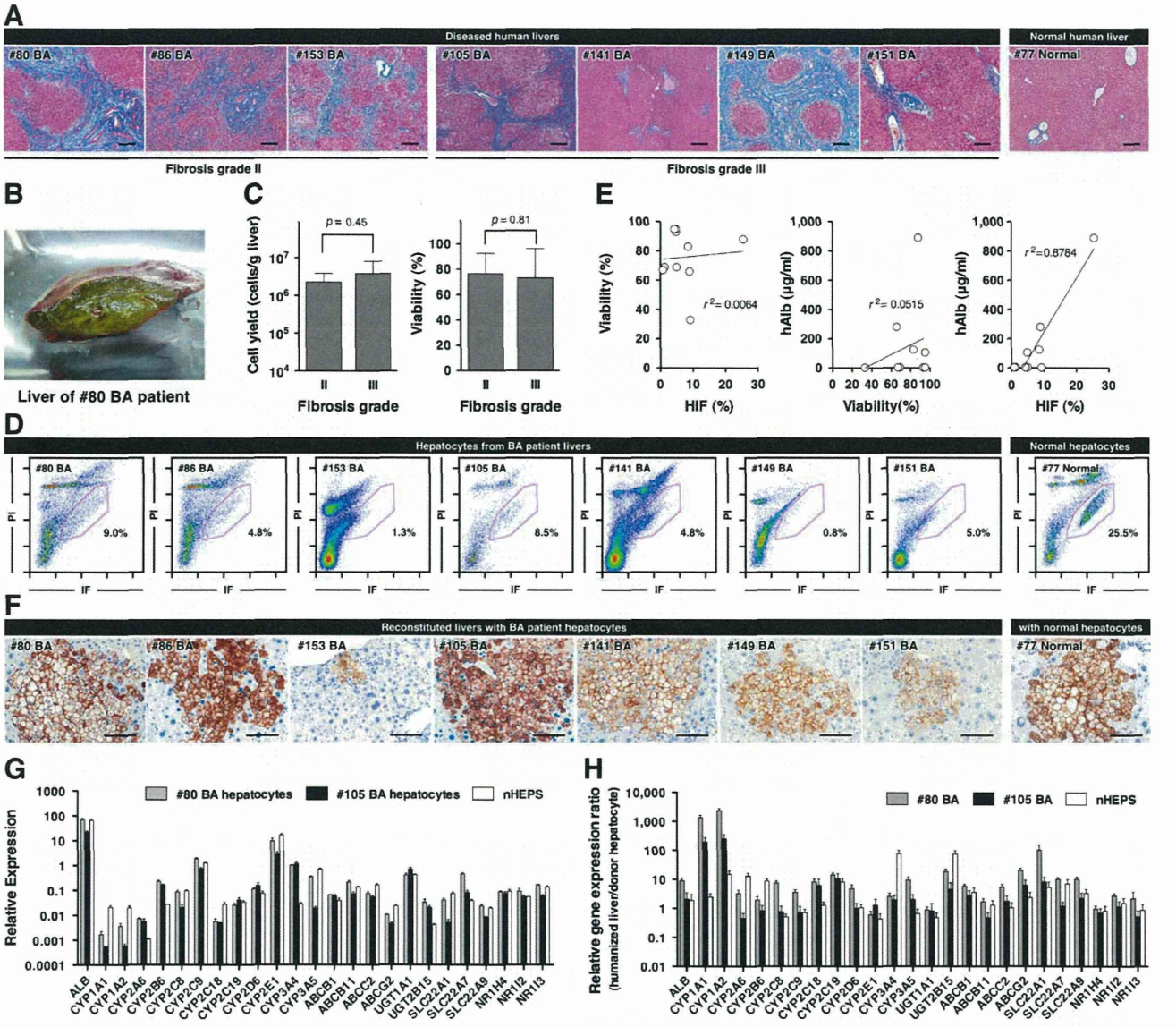

Figure 1. Engraftment of hepatocytes from BA patients in uPA-NOG mouse livers. (A) Azan-Mallory staining of 7 individual liver biopsy samples from BA patients and a healthy donor (normal). The scale bars represent 200 μm. (B) Gross morphology of the liver from BA patient 80. (C) Comparison of the cell yields and viability with grade II hepatic fibrosis and grade III hepatic fibrosis. (D) Isolated hepatocytes were analyzed with flow cytometry. Each HIF fraction is surrounded by a magenta border. (E) Correlation analyses of the cell viability, the HIF fraction percentage, and the hALB plasma concentration. (F) The engraftment of hepatocytes isolated from the BA patients and the healthy donors was confirmed with anti-human HLA staining. The scale bars represent 50 μm. (G) The relative expression levels of 24 human drug metabolism–related messenger RNAs in hepatocytes from BA patients and NHEPS hepatocytes were corrected with GAPDH. (H) The relative ratio of the gene expression for each reconstituted liver was referenced to the RNA extracted from the donor hepatocytes.

(Fig. 3A,B,). The cholestasis, visualized with Hall's bilirubin staining, was observed in many BCs in the livers of patients with BA (Fig. 3A, right). In contrast, the colonies repopulated with hepatocytes from patients with BA within the host mouse livers did not accumulate bile within their BCs (Fig. 3B). Azan-Mallory staining and VIM and αSMA antibody staining revealed fibrosis in the livers of patients with BA (Fig. 3C), but no fibrosis was observed within the colony repopulated with hepatocytes from patients with BA (Fig. 3D). We wondered whether these hepatocytes could reconstitute the functionally integrated BC network within the host mouse liver; therefore, we assessed the transporter function within the colonies of hepatocytes from patients with BA with 5-CFDA, a fluorescent marker used to visualize biliary excretion into BCs. After it is administered, 5-CFDA enters hepatocytes and is metabolized into 5-CF. This compound is excreted into BCs through the organic anion transporter MRP2.[27] Within the first 15 minutes after the administration of 5-CFDA, the hepatocytes from patients with BA in the uPA-NOG mice excreted 5-CF into the BCs, and it formed honeycomb networks surrounding individual hepatocytes (Fig. 4, top). This

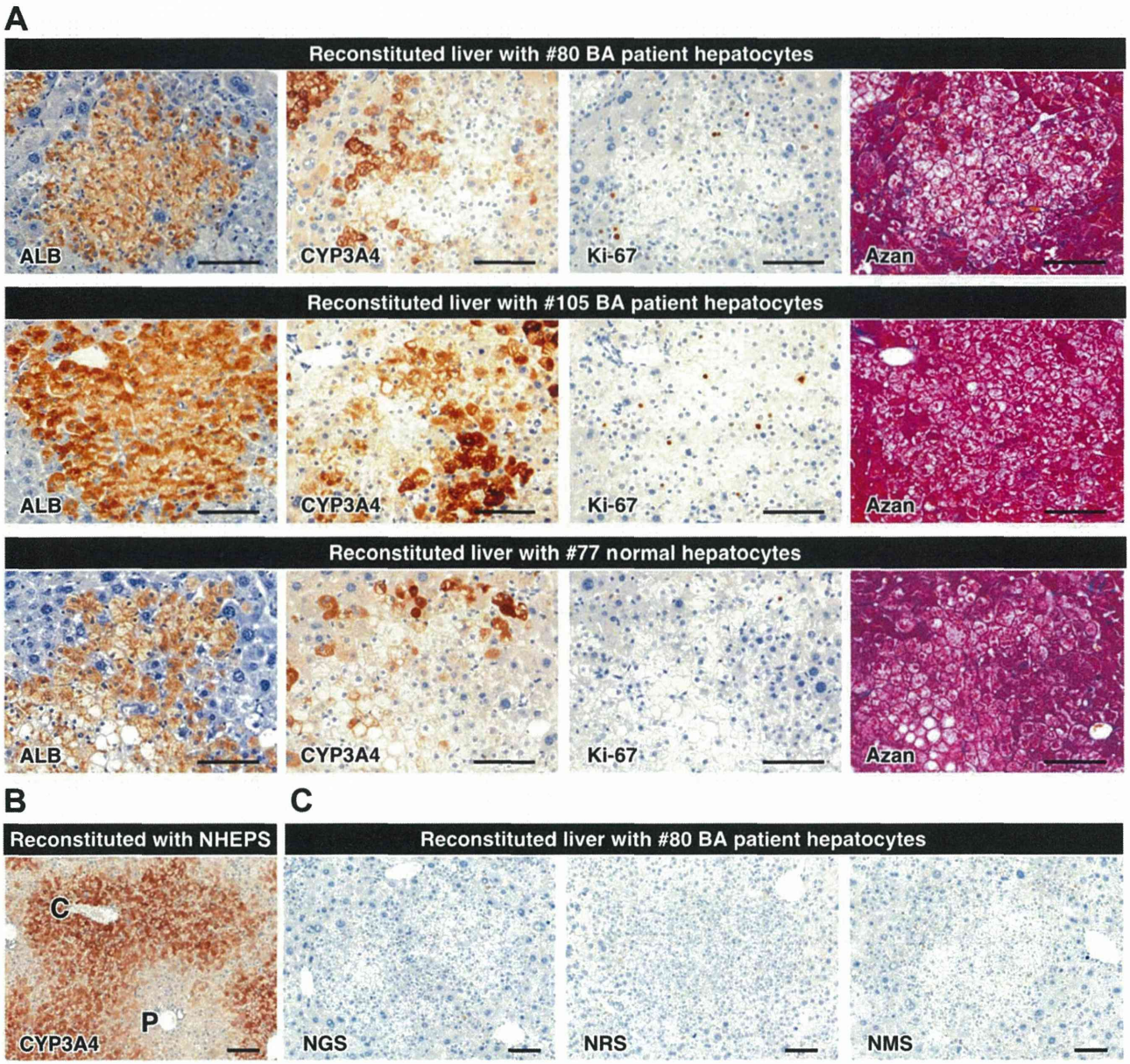

Figure 2. Immunohistochemistry of uPA-NOG mouse livers engrafted with BA patient hepatocytes. (A) Sections were stained for hALB, human CYP3A4, and human Ki-67 antigen; Azan-Mallory staining was also used. The scale bars represent 100 μm. (B) Immunohistochemical staining for CYP3A4 in a fully reconstituted uPA-NOG liver with NHEPS hepatocytes. The scale bar represents 100 μm. (C) Negative controls for immunostaining: NGS, NRS, and NMS. The scale bars represent 100 μm.

process was also observed in the colonies of NHEPS hepatocytes (Fig. 4, middle) but not in the HCT 116 colorectal tumors (Fig. 4, bottom). The typical BC network was detectable in the human hepatocyte conglomerates, as visualized by anti-MRP2, HLA antibodies, and H&E staining (Fig. 4). These results suggest that the intrahepatic bile duct system within the colonies reconstituted with hepatocytes from patients with BA must be nondefective.

DISCUSSION

BA is the most common reason for LT in children worldwide. The aim of this study was to evaluate regenerative medicine as a possible alternative to LT for treating BA. We succeeded in isolating viable hepatocytes from the livers of patients with BA so that we could evaluate the regenerative potential in vivo with a liver failure mouse model.[11] Recently, Gramignoli et al.[28] reported the successful isolation of hepatocytes from people with a number of different metabolic and other liver diseases (n = 35). The purpose of their study was to evaluate hepatocytes from individuals with metabolic disease for use in cell therapy via hepatocyte transplantation. Although they performed hepatocyte isolation in patients with BA (n = 7), those cells would not be recommended for clinical transplants because of concerns about cell yields, viability,

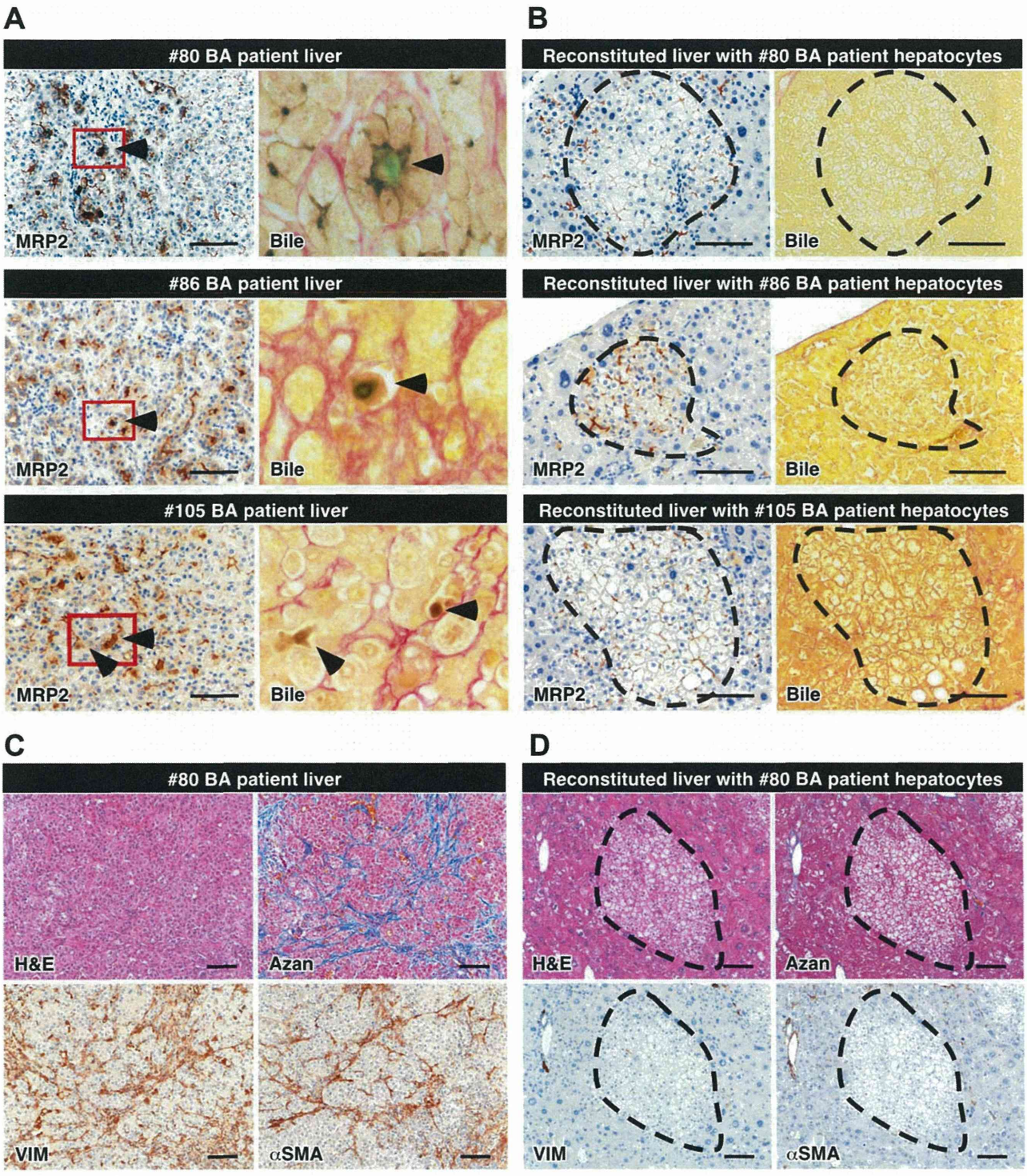

Figure 3. Detection of biliary obstructions and hepatic fibrosis. (A) Immunohistochemical staining for MRP2 protein in livers from patients with BA (patients 80, 86, and 105; left). Enlarged views of the boxed areas are shown with Hall's bilirubin staining (right). Bile stained with Hall's method appears green (arrowheads). (B) Immunohistochemical staining for MRP2 protein (left) and Hall's bilirubin staining (right) in uPA-NOG mouse livers engrafted with hepatocytes from BA patients (patients 80, 86, and 105). The dotted areas indicate the repopulated human liver. (C) H&E and Azan-Mallory staining and immunohistochemical staining for VIM and αSMA in the liver from a BA patient (patient 80). (D) H&E and Azan-Mallory staining and immunohistochemical staining for VIM and αSMA in a uPA-NOG mouse liver engrafted with hepatocytes from a BA patient (patient 80). The dotted areas indicate the repopulated human liver. The scale bars represent 100 μm.

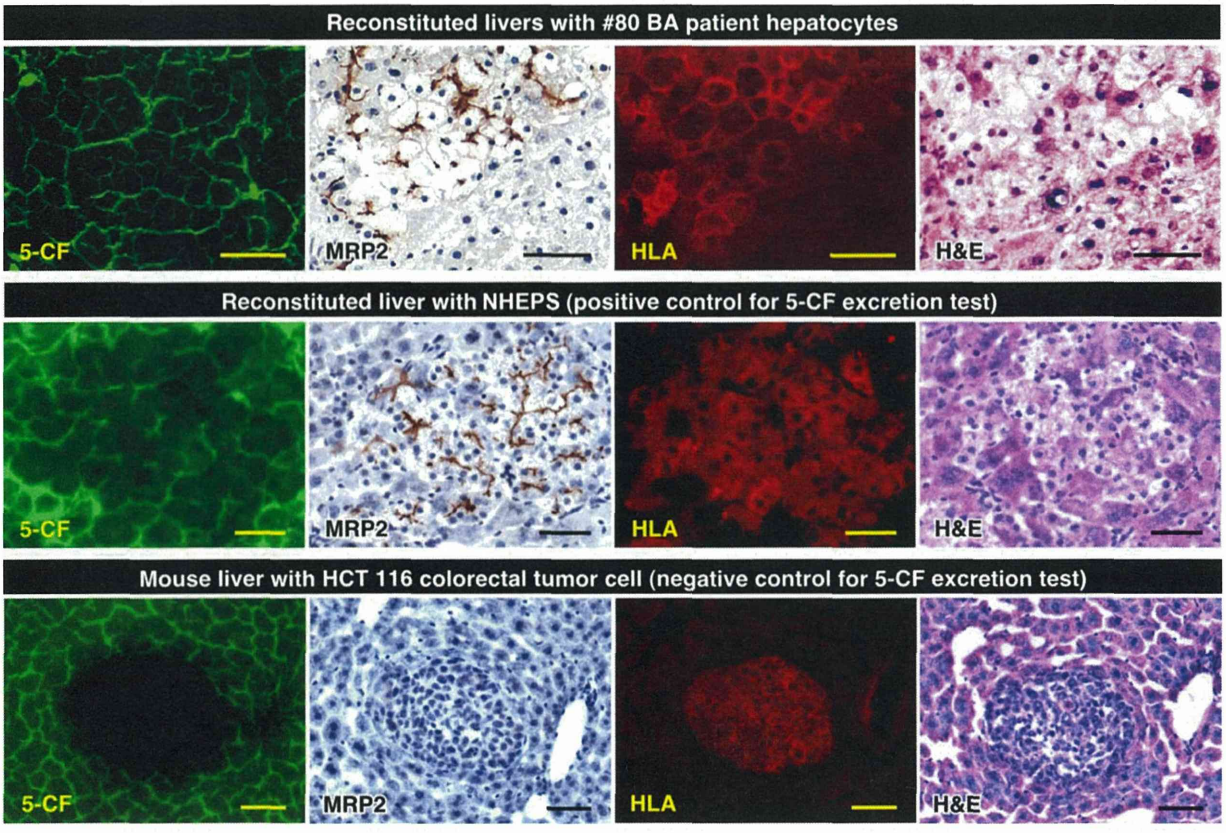

Figure 4. Functional integrity of the BC network within the reconstituted livers. Biliary excretion tests were performed with a fluorescent metabolic marker (5-CFDA). Serial sections were prepared from the livers of mice that received transplants of hepatocytes from a BA patient (patient 80), commercially available cryopreserved hepatocytes (NHEPS; positive control), or HCT 116 colorectal tumor cells (negative control). The sections were loaded with 5-CFDA, and the presence of the fluorescent metabolite 5-CF was assessed. In the livers reconstituted with patient hepatocytes and NHEPS hepatocytes, 5-CF (green on a dark field) was rapidly excreted into the BCs that formed the honeycomb networks over the lobule. In contrast, the BCs around the tumor, which formed after the transplantation of HCT 116 colorectal tumor cells, did not have this honeycomb pattern. Additional sections were stained for human MRP2 (brown in a bright field) and HLA (red in a dark field); H&E staining was also performed. The scale bars represent 50 μm.

and function. Bhogal et al.[29] reported that the viability, the total cell yield, and the success rate with cirrhotic tissues were low. In the current study, the cell yield and cell viability of hepatocytes from BA patients with fibrosis grade II or III were comparable to the yields and viability previously reported by Gramignoli et al. We expected that the low cell yield and viability would depend on the degree of fibrosis in patients with BA. However, there were no significant differences in the cell yields of hepatocytes from patients with grade II fibrosis and hepatocytes from patients with grade III fibrosis (Fig. 1C) or in cell viability (Fig. 1D). These results indicate that regardless of the extent of hepatic fibrosis, the presence of fibrosis affects the cell yield and viability when hepatocytes are isolated from the livers of patients with BA.

For hepatocytes from patient 80, 3 different conditions (freshly isolated, chilled, and frozen-thawed hepatocytes) were compared in terms of their engraftment and proliferative potential in a liver failure model using uPA-NOG mice. HLA-positive hepatocyte colonies were observed in the livers of all uPA-NOG mice that underwent transplantation with hepatocytes of any condition; however, a higher ratio of hALB-secreting mice and a higher level of serum hALB were observed in the mice that underwent transplantation with freshly isolated hepatocytes (Table 2). We succeeded in isolating a small number of hepatocytes buried in the severely cirrhotic liver of BA patient 149 (fibrosis grade III), and surprisingly, the hepatocytes could successfully engraft and proliferate within the uPA-NOG mouse livers as HLA-positive colonies. These results indicate that even hepatocytes buried in the cirrhotic livers of patients with BA do not lose their proliferative potential.

Recent studies of the molecular biology of BA have revealed no significant differences in the hepatic MRP2 expression levels of BA patients and control groups.[30] In fact, we confirmed the expression of not only the adenosine triphosphate–binding cassette, subfamily C (cystic fibrosis transmembrane conductance regulator (CFTR)/multidrug resistance-associated protein (MRP)), member 2 (ABCC2) gene but also the MRP2 protein, which was located on the apical plasma membranes of hepatocytes both in the livers of BA patients (Fig. 3A, left) and in partially humanized livers repopulated with hepatocytes from patients

with BA (Fig. 3B, left). Despite the normal MRP2 protein expression in the livers of patients with BA and in the partially humanized mouse liver, the bile was accumulated only in the many BCs of livers from patients with BA. This result clearly demonstrates the extrahepatic obstruction of the biliary flow.

In this study, using a reconstituted-liver mouse model, we examined the hepatocytes of patients with BA for the presence of abnormalities in vivo. Unfortunately, we failed to establish a BA model with liver-injured mice. However, this result indicates that the primary etiology of BA is absent in the hepatocytes themselves, and the hepatocytes buried in the cirrhotic livers of patients with BA are functionally intact hepatocytes retaining their proliferative potential and able to reconstitute a partially functioning human liver in mice. Gramignoli et al.[28] recently reported the isolation of hepatocytes from patients with many metabolic diseases, including BA, and the rapid and efficient repopulation of FRG (fumarylacetoacetate hydrolase (Fah), recombination activating gene 2 (Rag2) and interleukin 2 receptor gamma chain (Il-2rγ) triple gene knockout) mouse livers after the transplantation of hepatocytes obtained from patients with metabolic disease. In addition to Gramignoli et al.'s report, the current study supports the hypothesis that hepatocytes from patients with BA are morphologically and biochemically normal.

Recently, it has been reported that the extent of liver fibrosis at the time of portoenterostomy, as evaluated by picrosirius red staining, appears to be a strong negative predictor of outcomes.[31] The negative correlation between the extent of liver fibrosis and the yield of viable hepatocytes suggested by our results might be associated with that phenomenon. These results support the possibility that if the primary etiology is removed by Kasai portoenterostomy before progressive cholestasis develops, the liver of the patient with BA may regenerate autologously via the functionally intact hepatocytes remaining in the cirrhotic liver. The hepatocyte function in patients with BA may be independent of the degree of fibrosis; therefore, efforts to ameliorate the fibrosis would have great promise in treating this disease. Treatment would include an earlier diagnosis and surgery but might also include developing antifibrotic pharmacological approaches. If a method for earlier diagnosis or new drugs are developed in the near future, patients with BA may not require an operation that is as difficult as LT.

ACKNOWLEDGMENT

The authors thank M. Kuronuma, Y. Ando, T. Ogura, T. Kamisako, and R. Takahashi for their outstanding technical assistance with the animal experiments. They also thank M. Yamamoto, H. Nabekawa, and C. Kito for their technical assistance with molecular analyses and Dr. M. Ito, S. Enosawa, and M. Onodera for their helpful discussions.

REFERENCES

1. Hartley JL, Davenport M, Kelly DA. Biliary atresia. Lancet 2009;374:1704-1713.
2. Bassett MD, Murray KF. Biliary atresia: recent progress. J Clin Gastroenterol 2008;42:720-729.
3. Muratore CS, Harty MW, Papa EF, Tracy TF Jr. Dexamethasone alters the hepatic inflammatory cellular profile without changes in matrix degradation during liver repair following biliary decompression. J Surg Res 2009; 156:231-239.
4. Sokol RJ, Shepherd RW, Superina R, Bezerra JA, Robuck P, Hoofnagle JH. Screening and outcomes in biliary atresia: summary of a National Institutes of Health workshop. Hepatology 2007;46:566-581.
5. Serinet MO, Wildhaber BE, Broué P, Lachaux A, Sarles J, Jacquemin E, et al. Impact of age at Kasai operation on its results in late childhood and adolescence: a rational basis for biliary atresia screening. Pediatrics 2009;123: 1280-1286.
6. Czech-Schmidt G, Verhagen W, Szavay P, Leonhardt J, Petersen C. Immunological gap in the infectious animal model for biliary atresia. J Surg Res 2001;101:62-67.
7. Petersen C, Biermanns D, Kuske M, Schäkel K, Meyer-Junghänel L, Mildenberger H. New aspects in a murine model for extrahepatic biliary atresia. J Pediatr Surg 1997;32:1190-1195.
8. Riepenhoff-Talty M, Schaekel K, Clark HF, Mueller W, Uhnoo I, Rossi T, et al. Group A rotaviruses produce extrahepatic biliary obstruction in orally inoculated newborn mice. Pediatr Res 1993;33(pt 1):394-399.
9. Dandri M, Burda MR, Török E, Pollok JM, Iwanska A, Sommer G, et al. Repopulation of mouse liver with human hepatocytes and in vivo infection with hepatitis B virus. Hepatology 2001;33:981-988.
10. Mercer DF, Schiller DE, Elliott JF, Douglas DN, Hao C, Rinfret A, et al. Hepatitis C virus replication in mice with chimeric human livers. Nat Med 2001;7:927-933.
11. Suemizu H, Hasegawa M, Kawai K, Taniguchi K, Monnai M, Wakui M, et al. Establishment of a humanized model of liver using NOD/Shi-scid IL2Rgnull mice. Biochem Biophys Res Commun 2008;377:248-252.
12. Barshes NR, Lee TC, Udell IW, O'Mahoney CA, Karpen SJ, Carter BA, Goss JA. The Pediatric End-Stage Liver Disease (PELD) model as a predictor of survival benefit and posttransplant survival in pediatric liver transplant recipients. Liver Transpl 2006;12:475-480.
13. Weerasooriya VS, White FV, Shepherd RW. Hepatic fibrosis and survival in biliary atresia. J Pediatr 2004;144: 123-125.
14. Seglen PO. Preparation of isolated rat liver cells. Methods Cell Biol 1976;13:29-83.
15. Miyamoto Y, Suzuki S, Nomura K, Enosawa S. Improvement of hepatocyte viability after cryopreservation by supplementation of long-chain oligosaccharide in the freezing medium in rats and humans. Cell Transplant 2006;15:911-919.
16. Nakamura K, Mizutani R, Sanbe A, Enosawa S, Kasahara M, Nakagawa A, et al. Evaluation of drug toxicity with hepatocytes cultured in a micro-space cell culture system. J Biosci Bioeng 2011;111:78-84.
17. Hasegawa M, Kawai K, Mitsui T, Taniguchi K, Monnai M, Wakui M, et al. The reconstituted 'humanized liver' in TK-NOG mice is mature and functional. Biochem Biophys Res Commun 2011;405:405-410.
18. Tsukahara T, Kawaguchi S, Torigoe T, Asanuma H, Nakazawa E, Shimozawa K, et al. Prognostic significance of HLA class I expression in osteosarcoma defined by anti-pan HLA class I monoclonal antibody, EMR8-5. Cancer Sci 2006;97:1374-1380.

19. Key G, Becker MH, Baron B, Duchrow M, Schlüter C, Flad HD, Gerdes J. New Ki-67-equivalent murine monoclonal antibodies (MIB 1-3) generated against bacterially expressed parts of the Ki-67 cDNA containing three 62 base pair repetitive elements encoding for the Ki-67 epitope. Lab Invest 1993;68:629-636.
20. Scheffer GL, Kool M, Heijn M, de Haas M, Pijnenborg AC, Wijnholds J, et al. Specific detection of multidrug resistance proteins MRP1, MRP2, MRP3, MRP5, and MDR3 P-glycoprotein with a panel of monoclonal antibodies. Cancer Res 2000;60:5269-5277.
21. Dekel B, Shezen E, Even-Tov-Friedman S, Katchman H, Margalit R, Nagler A, Reisner Y. Transplantation of human hematopoietic stem cells into ischemic and growing kidneys suggests a role in vasculogenesis but not tubulogenesis. Stem Cells 2006;24:1185-1193.
22. Skalli O, Ropraz P, Trzeciak A, Benzonana G, Gillessen D, Gabbiani G. A monoclonal antibody against alpha-smooth muscle actin: a new probe for smooth muscle differentiation. J Cell Biol 1986;103(pt 2):2787-2796.
23. Hall MJ. A staining reaction for bilirubin in sections of tissue. Am J Clin Pathol 1960;34:313-316.
24. Hamada K, Monnai M, Kawai K, Nishime C, Kito C, Miyazaki N, et al. Liver metastasis models of colon cancer for evaluation of drug efficacy using NOD/Shi-scid IL2R-gammanull (NOG) mice. Int J Oncol 2008;32:153-159.
25. Limas C, Bigler A, Bair R, Bernhart P, Reddy P. Proliferative activity of urothelial neoplasms: comparison of BrdU incorporation, Ki67 expression, and nucleolar organiser regions. J Clin Pathol 1993;46:159-165.
26. Mills SJ, Shepherd NA, Hall PA, Hastings A, Mathers JC, Gunn A. Proliferative compartment deregulation in the non-neoplastic colonic epithelium of familial adenomatous polyposis. Gut 1995;36:391-394.
27. Kudo A, Kashiwagi S, Kajimura M, Yoshimura Y, Uchida K, Arii S, Suematsu M. Kupffer cells alter organic anion transport through multidrug resistance protein 2 in the post-cold ischemic rat liver. Hepatology 2004;39:1099-1109.
28. Gramignoli R, Tahan V, Dorko K, Skvorak KJ, Hansel MC, Zhao W, et al. New potential cell source for hepatocyte transplantation: discarded livers from metabolic disease liver transplants. Stem Cell Res 2013;11:563-573.
29. Bhogal RH, Hodson J, Bartlett DC, Weston CJ, Curbishley SM, Haughton E, et al. Isolation of primary human hepatocytes from normal and diseased liver tissue: a one hundred liver experience. PLoS One 2011;6:e18222.
30. Terui K, Saito T, Hishiki T, Sato Y, Mitsunaga T, Yoshida H. Hepatic expression of multidrug resistance protein 2 in biliary atresia. Comp Hepatol 2011;10:6.
31. Pape L, Olsson K, Petersen C, von Wasilewski R, Melter M. Prognostic value of computerized quantification of liver fibrosis in children with biliary atresia. Liver Transpl 2009;15:876-882.

OPEN

Citation: Blood Cancer Journal (2014) 4, e226; doi:10.1038/bcj.2014.47

www.nature.com/bcj

ORIGINAL ARTICLE

Prognostic implications of *CEBPA* mutations in pediatric acute myeloid leukemia: a report from the Japanese Pediatric Leukemia/Lymphoma Study Group

H Matsuo[1], M Kajihara[1], D Tomizawa[2], T Watanabe[3], AM Saito[4], J Fujimoto[5], K Horibe[4], K Kodama[1], M Tokumasu[6], H Itoh[1], H Nakayama[7], A Kinoshita[8], T Taga[9], A Tawa[10], T Taki[11], S Tanaka[12] and S Adachi[1]

CCAAT/enhancer-binding protein alpha (*CEBPA*) mutations are a favorable prognostic factor in adult acute myeloid leukemia (AML) patients; however, few studies have examined their significance in pediatric AML patients. Here we examined the *CEBPA* mutation status and clinical outcomes of pediatric AML patients treated in the AML-05 study. We found that 47 (14.9%) of the 315 evaluable patients harbored mutations in *CEBPA*; 26 cases (8.3%) harbored a single mutation (*CEBPA*-single) and 21 (6.7%) harbored double or triple mutations (*CEBPA*-double). After excluding core-binding factor-AML cases, patients harboring *CEBPA* mutations showed better overall survival (OS; $P = 0.048$), but not event-free survival (EFS; $P = 0.051$), than wild-type patients. Multivariate analysis identified *CEBPA*-single and *CEBPA*-double as independent favorable prognostic factors for EFS in the total cohort (hazard ratio (HR): 0.47 and 0.33; $P = 0.02$ and 0.01, respectively). *CEBPA*-double was also an independent favorable prognostic factor for OS (HR: 0.30; $P = 0.04$). *CEBPA*-double remained an independent favorable factor for EFS (HR: 0.28; $P = 0.04$) in the normal karyotype cohort. These results suggest that *CEBPA* mutations, particularly *CEBPA*-double, are an independent favorable prognostic factor in pediatric AML patients, which will have important implications for risk-stratified therapy.

Blood Cancer Journal (2014) **4,** e226; doi:10.1038/bcj.2014.47; published online 11 July 2014

INTRODUCTION

CCAAT/enhancer-binding protein alpha (CEBPA) is a transcription factor that co-ordinates cellular differentiation. CEBPA is expressed in myeloid precursors during hematopoiesis, where it regulates the expression of several granulocyte-specific genes.[1] CEBPA inhibits E2F pathways, thereby downregulating c-Myc and allowing myeloid precursors to enter the granulocytic differentiation pathway.[2,3] The *CEBPA* gene is located on chromosome 19 band q13.1. Approximately 10% of acute myeloid leukemia (AML) patients harbor mutations in *CEBPA* genes, and these mutations can occur across the whole gene, but there are two main hotspots.[4,5] N-terminal out-of-frame mutations are located between the major translational start site and a second ATG further downstream. They abolish translation of the full-length p42 isoform of CEBPA, leading to overexpression of a shorter dominant-negative p30 isoform.[6] C-terminal mutations are generally in-frame insertions/deletions located in the basic leucine zipper (bZIP) domain; these mutations disrupt binding to DNA or dimerization.[7] Most AML patients with double *CEBPA* mutations harbor both N- and C-terminal mutations, which are typically present on different alleles; however, homozygous mutations have also been described.[8]

CEBPA mutations are a favorable prognostic factor for AML, particularly in patients harboring double *CEBPA* mutations and a normal karyotype.[8–13] However, the prognostic value of *CEBPA* mutations has been studied mostly in adult AML patients, with few studies examining mutations in pediatric AML patients. The first set of pediatric data was presented by the Taiwan Pediatric Oncology Group, but the report lacked data regarding clinical outcome.[14] The prognostic impact of *CEBPA* in pediatric AML was reported by two other groups, namely, the Children's Oncology Group and the Dutch Childhood Oncology Group/the Berlin–Frankfurt–Münster Study Group,[15,16] which both reported that, after excluding core-binding factor (CBF)-AML cases, patients harboring *CEBPA* mutations had a significantly better clinical outcome than those harboring the wild-type (WT) gene; however, the clinical implications of single vs double mutations were unclear. A more recent study conducted by the Nordic Society of Pediatric Hematology and Oncology suggests that *CEBPA* mutations in pediatric AML patients are not associated with improved survival;[17] thus the clinical significance of *CEBPA* mutations in pediatric AML patients is unclear. Although we previously reported the characteristics of *CEBPA* mutations in Japanese children with AML, the small sample size meant that further study was required.[18]

Here we examined the *CEBPA* mutation status and clinical outcomes of pediatric AML patients treated in the Japanese Pediatric Leukemia/Lymphoma Study Group (JPLSG) AML-05 study.

[1]Department of Human Health Sciences, Kyoto University, Kyoto, Japan; [2]Department of Pediatrics, Tokyo Medical and Dental University (TMDU), Tokyo, Japan; [3]Department of Nutritional Science, Aichi Gakuin University, Aichi, Japan; [4]Clinical Research Center, National Hospital Organization Nagoya Medical Center, Aichi, Japan; [5]Clinical Research Center, National Center for Child Health and Development, Tokyo, Japan; [6]Department of Pediatrics, Kyoto University, Kyoto, Japan; [7]Department of Pediatrics, National Hospital Organization Fukuoka-Higashi Medical Center, Fukuoka, Japan; [8]Department of Pediatrics, St Marianna University School of Medicine, Kanagawa, Japan; [9]Department of Pediatrics, Shiga University of Medical Science, Shiga, Japan; [10]Department of Pediatrics, National Hospital Organization Osaka Medical Hospital, Osaka, Japan; [11]Department of Molecular Diagnostics and Therapeutics, Kyoto Prefectural University of Medicine, Kyoto, Japan and [12]Department of Pharmacoepidemiology, Kyoto University, Kyoto, Japan. Correspondence: Professor S Adachi, Department of Human Health Sciences, Graduate School of Medicine, Kyoto University, 53 Kawahara-cho, Syogoin, Sakyoku, Kyoto 606-8507, Japan.
E-mail: adachiso@kuhp.kyoto-u.ac.jp
Received 4 May 2014; accepted 19 May 2014

SUBJECTS AND METHODS

Patients and study protocol

The AML-05 study is a Japanese nationwide multi-institutional study of children (age <18 years) with *de novo* AML, all of whom were enrolled between 1 November 2006 and 31 December 2010. The trial is registered with the UMIN Clinical Trials Registry (UMIN-CTR; http://www.umin.ac.jp/ctr/index.htm; number UMIN000000511).

In all, 485 patients with suspected AML (diagnosed at 118 centers and hospitals in Japan) were registered in the AML-05 study. Patients with acute promyelocytic leukemia, Down's syndrome, secondary AML, myeloid/natural killer cell leukemia and myeloid sarcoma, were not eligible. Overall, 38 patients were excluded, mainly because of misdiagnosis, while four additional patients were excluded for the following reasons: the patient's guardian refused permission to participate ($n=1$); there was a significant protocol violation during the initial induction course ($n=1$); the hospital withdrew from the JPLSG ($n=1$); and the patient was transferred to a non-JPLSG member hospital ($n=1$). Patients were stratified into three risk groups according to specific cytogenetic characteristics and morphological responses to treatment. CBF-AML patients were assigned to the low-risk group; those with unfavorable cytogenetics (-7, 5q-, t(16;21)(p11;q22), Ph1, Fms-like tyrosine kinase 3 internal tandem duplications (*FLT3*-ITD)) and poor induction responders were assigned to the high-risk group; and the rest were assigned to the intermediate-risk group. Details of the patient disposition, treatment schedules and risk stratification have been described previously.[19,20] In the present study, morphology was diagnosed prospectively using a central review system. Cytogenetic tests were performed in regional laboratories, but the reports were reviewed centrally. The study was conducted in accordance with the principles set down in the Declaration of Helsinki and was approved by the Ethics Committees of all participating institutions. All patients, or the patients' parents/guardians, provided written informed consent.

Mutation analysis

cDNA was synthesized from RNA obtained from diagnostic bone marrow samples using the Omniscript Reverse Transcription Kit (Qiagen, Chatsworth, CA, USA), according to the manufacturer's recommendations. The entire coding region of the *CEBPA* gene was amplified using the overlapping PCR primer pairs followed by direct sequencing, as previously described.[6,18]

Statistical analysis

Patient characteristics were analyzed using Fisher's exact test (categorical variables) and the Kruskal–Wallis test (continuous variables). Event-free survival (EFS) was defined as the time from the diagnosis of AML to the last follow-up or the first event (failure to achieve remission, relapse, secondary malignancy or any-cause death). Overall survival (OS) was defined as the time from the diagnosis of AML to any-cause death. The Kaplan–Meier method was used to estimate EFS and OS, and data were compared using the log-rank test. To determine the prognostic value of *CEBPA* mutation, Cox regression analysis was performed using SAS version 9.2 (SAS Institute Inc., Cary, NC, USA). All tests were two-tailed, and a *P*-value <0.05 was considered statistically significant.

RESULTS

Mutation analysis

Diagnostic samples from 315/443 (71.1%) eligible AML patients were analyzed for *CEBPA* mutations; *CEBPA* data were unavailable for 128 patients. There were no significant differences in the major characteristics or clinical outcomes of the 315 patients and the 128 patients for whom no data were available (EFS $P=0.78$, OS $P=0.30$). We found that 47/315 patients (14.9%) harbored a mutation in *CEBPA*, 26 (8.3%) harbored a single mutation and 21 (6.7%) harbored double or triple mutations. The location and combination pattern of all the detected mutations are shown in Figure 1 and Table 1. Single mutations were distributed across the entire gene, but most in-frame insertions/deletions were located in the bZIP domain. By contrast, double or triple mutations were clustered in the N- and C-terminal hotspots. Thirteen out of the 21 cases (61.9%) harbored both an N-terminal out-of-frame mutation and an in-frame mutation in the bZIP domain, which were predicted to result in a lack of WT CEBPA p42 expression. We identified five patients with triple mutations but could not exclude the possibility that these mutations occurred in different cells. Moreover, the method we used cannot identify whether mutations are located on different alleles. Further study is required to overcome these limitations.

Polymorphisms in the *CEBPA* mutations

Overall, 131 patients (41.6%) harbored an in-frame 6-bp insertion (ACCCGC) in the transactivation domain 2 (TAD2), resulting in a His-Pro duplication (HP196–197 insertion). This mutation is observed in approximately 10% of healthy controls and AML patients and is reported as a germline polymorphism.[21,22] We did not identify any differences in characteristics between the HP196–197 insertion-positive and -negative groups, and the clinical outcomes of both groups were similar (data not shown). Therefore, we ignored this mutation during our analysis of clinical outcome, along with other mutations that did not result in amino-acid changes.

Patient characteristics

Patient characteristics according to *CEBPA* mutation status are shown in Table 2. Patients harboring a single *CEBPA* mutation were described as '*CEBPA*-single' and those harboring double or triple *CEBPA* mutations were described as '*CEBPA*-double'. *CEBPA*-double patients showed a significantly higher percentage of M1 or M2 French–American–British subtypes ($P<0.001$). Compared with WT patients, patients with *CEBPA* mutations were older ($P=0.03$) at the time of diagnosis. *CEBPA* mutations were predominant in those with an intermediate risk ($P=0.002$) and a normal karyotype ($P<0.001$). There was a well-balanced gender distribution ($P=0.84$), and there were no significant differences in the number of patients with *FLT3*-ITD and *NPM1* mutations among the three *CEBPA* subgroups.

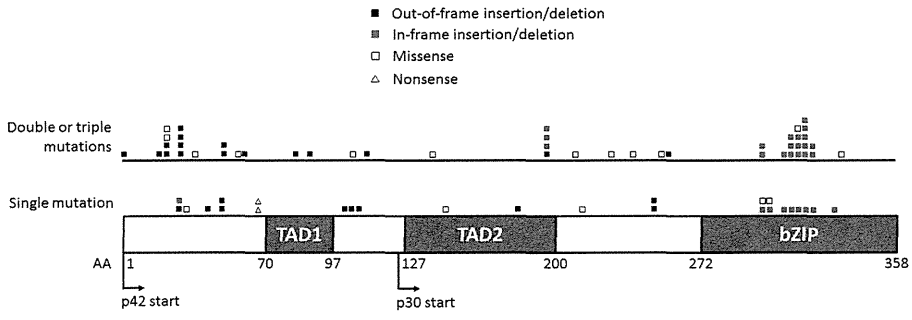

Figure 1. Location and type of the mutations detected in pediatric AML patients enrolled in the AML-05 study. AA, amino acid; BZIP, basic leucine zipper; TAD, transactivation domain.

Table 1. Summary of *CEBPA* mutations detected in 315 acute myeloid leukemia patients

Mutation status	*Mutation 1*			*Mutation 2 (Mutation 3)*			
	N-terminal AA 1-120	*Middle* AA 121-277	*C-terminal* AA 278-358	*N-terminal* AA 1-120	*Middle* AA 121-277	*C-terminal* AA 278-358	*No. of patients*
CEBPA-single	Out-of-frame ins/del						7
	In-frame ins/del						1
	Missense						1
	Nonsense						2
		Out-of-frame ins/del					3
		Missense					2
			In-frame ins/del				8
			Missense				2
Total							26
CEBPA-double	Out-of-frame ins/del					In-frame ins/del	11
	Missense			Missense			1
	Missense				Missense		1
	Missense					Missense	1
		Out-of-frame ins/del				In-frame ins/del	2
	Out-of-frame ins/del			Missense	(In-frame ins/del)		1
	Out-of-frame ins/del				In-frame ins/del	(In-frame ins/del)	2
		Missense			Missense (Missense)		1
		Missense				Missense (In-frame ins/del)	1
Total							21

Abbreviations: AA, amino acid; *CEBPA*, CCAAT/enhancer-binding protein alpha; del, deletion; ins, insertion. Note: Patients harboring a single *CEBPA* mutation were described as *CEBPA*-single and those harboring double or triple *CEBPA* mutations were described as *CEBPA*-double.

Prognostic impact of *CEBPA* in the total cohort

We first analyzed the clinical outcomes of patients harboring *CEBPA* mutations and then compared them with the outcomes of CBF-AML patients and patients without CBF or *CEBPA* mutations (denoted 'WT non-CBF') (Figure 2). The CBF-AML group included AML patients harboring t(8;21)(q22;q22) along with inv(16)(p13.1q22) or its variant t(16;16)(p13.1;q22). Seven CBF-AML patients harboring *CEBPA* mutations were categorized as '*CEBPA*-mutant'. Patients harboring *CEBPA* mutations showed better OS ($P=0.048$), but not EFS ($P=0.051$), than WT non-CBF patients (Figures 2a and b). However, patients with *CEBPA* mutations showed poorer OS ($P=0.0006$) than patients with CBF-AML. Furthermore, we examined whether the number of *CEBPA* mutations had an impact on prognosis (Figures 2c and d). *CEBPA*-double patients did not show significantly better EFS and OS than *CEBPA*-single patients ($P=0.33$ each). There was also no significant difference in EFS and OS between *CEBPA*-double patients and WT non-CBF patients ($P=0.055$ and $P=0.057$, respectively).

Prognostic impact of *CEBPA* in the normal karyotype cohort

We next examined prognosis in the normal karyotype cohort, because *CEBPA* mutations have been described as a favorable prognostic factor, particularly in cytogenetically normal AML (Figure 3). There was no significant difference in EFS and OS between *CEBPA*-double patients and WT or *CEBPA*-single patients (EFS: *CEBPA*-double vs WT, $P=0.15$; *CEBPA*-double vs *CEBPA*-single, $P=0.21$; OS: *CEBPA*-double vs WT, $P=0.28$; *CEBPA*-double vs *CEBPA*-single; $P=0.44$). Patients with *CEBPA*-single showed almost identical EFS ($P=0.97$) and OS ($P=0.77$) to those of WT patients.

Prognostic impact of *CEBPA* mutation type

We also examined the prognostic impact of the location of the *CEBPA* mutations, which has never been examined in pediatric AML patients. Only patients with hotspot mutations predicted to cause translation of the p30 isoform and/or disruption or loss of the C-terminal bZIP domain were included in the analysis. In the total cohort, patients with an N-terminal out-of-frame mutation and a C-terminal in-frame mutation ($n=13$, denoted as *CEBPA*-double N + C-term) had significantly better EFS ($P=0.01$), but not OS ($P=0.06$), than WT non-CBF patients (Figures 4a and b). This patient group also had significantly better EFS, but not OS, than other *CEBPA*-double patients ($n=8$), suggesting that a combination of N-terminal and C-terminal mutations results in a better prognosis for *CEBPA*-double patients (data not shown). We also investigated differences in outcome between *CEBPA*-single patients with an N-terminal mutation and those with a C-terminal mutation and found that the clinical outcomes were nearly identical. In the normal karyotype cohort, we found no significant difference in the outcome of four groups: patients with an N-terminal out-of-frame mutation, patients with a C-terminal in-frame mutation, patients with an N-terminal out-of-frame mutation and a C-terminal in-frame mutation, and WT patients, which may be due to the small sample size (Figures 4c and d).

Multivariate analysis

Multivariate Cox regression analysis, including age and white blood cell count at the time of diagnosis, was performed to examine whether *CEBPA* mutations were a favorable prognostic factor (Table 3). *FLT3*-ITD and *NPM1* mutations were not included as variables owing to the small number of positive cases and

Table 2. Characteristics of patients categorized according to *CEBPA* mutation status

	Total	*WT*	*CEBPA-single*	*CEBPA-double*	P-*value*
Number	315	268	26	21	
Age, years					0.03[b]
Median	7.9	7.6	9.9	9.6	
Range	0.0–17.5	0.0–17.5	0.3–16.2	1.3–15.9	
Sex, n *(%)*					0.84[a]
Male	167 (53)	144 (54)	13 (50)	10 (48)	
Female	148 (47)	124 (46)	13 (50)	11 (52)	
WBC ($\times 10^9$/*l*)					0.052[b]
Median	57.8	52.6	58.1	124	
Range	0.8–985	0.8–552	1.9–381	3.9–985	
Risk groups, n *(%)*					0.002[a]
Low	87 (28)	81 (30)	4 (15)	2 (10)	
Intermediate	132 (42)	101 (38)	15 (58)	16 (76)	
High	43 (14)	37 (14)	6 (23)	0 (0)	
Unclassified	53 (17)	49 (18)	1 (4)	3 (14)	
FAB, n *(%)*					<0.001[a]
M0	7 (2)	7 (3)	0 (0)	0 (0)	
M1	43 (14)	28 (10)	5 (19)	10 (48)	
M2	79 (25)	63 (24)	9 (35)	7 (33)	
M4	52 (17)	46 (17)	6 (23)	0 (0)	
M5	70 (22)	67 (25)	1 (4)	2 (10)	
M6	8 (3)	5 (2)	2 (8)	1 (5)	
M7	31 (10)	29 (11)	2 (8)	0 (0)	
RAEB-T	25 (8)	23 (9)	1 (4)	1 (5)	
Karyotype, n *(%)*					<0.001[a]
Normal	62 (20)	35 (13)	14 (54)	13 (62)	
t(8;21)	75 (24)	69 (26)	3 (12)	3 (14)	
inv(16)	25 (8)	24 (9)	1 (4)	0 (0)	
11q23	48 (15)	47 (18)	0 (0)	1 (5)	
other	105 (33)	93 (35)	8 (31)	4 (19)	
Molecular abnormalities, n *(%)*					
FLT3-ITD	42 (13)	35 (13)	6 (23)	1 (5)	0.21[a]
NPM1	12/167 (7)	10/128 (8)	2/22 (9)	0/17 (0)	0.59[a]

Abbreviations: *CEBPA*, CCAAT/enhancer-binding protein alpha; FAB, French–American–British; *FLT3*-ITD, Fms-like tyrosine kinase 3 internal tandem duplications; *NPM1*, nucleophosmin; WBC, white blood cell count; WT, wild type. [a]Fisher's exact test. [b]Kruskal–Wallis test.

because no statistically significant differences were detected by univariate analysis. For the total cohort ($n=315$), multivariate analysis identified both *CEBPA*-single and *CEBPA*-double as independent favorable prognostic factors for EFS (hazard ratio (HR): 0.47 and 0.33; $P=0.02$ and 0.01, respectively; upper column, Table 3). C*EBPA*-double was also identified as an independent favorable prognostic factor for OS (HR: 0.30; $P=0.04$). For the normal karyotype cohort ($n=62$), *CEBPA*-double was also identified as an independent prognostic factor for favorable EFS (HR: 0.28; $P=0.04$; lower column, Table 3). This may indicate that other factors, such as age and white blood cell count, had masked the benefit of *CEBPA* mutations in the univariate analysis.

DISCUSSION

Here we examined *CEBPA* mutations in 315 pediatric AML patients enrolled in the AML-05 study. We detected *CEBPA* mutations in 47 patients (14.9%), which is comparable to the reported frequency in adult and pediatric AML patients (approximately 10%).[8–17] In all, 26 out of the 47 cases (55.3%) harbored a single *CEBPA* mutation; this percentage is higher than that reported in previous studies of pediatric AML patients.[15,16] We detected the HP196–197 insertion in 131/315 cases (41.6%). This well-known polymorphism was previously observed in approximately 10% of AML cases; thus the percentage identified in the present study was rather high.[21,22] Whether this polymorphism is also common in healthy Japanese populations remains to be seen. A recent study by a Korean group reported the incidence of this polymorphism as 30%; thus the frequency of this polymorphism may vary considerably according to geographical region.[23] The majority of *CEBPA*-double patients comprised M1 or M2 French–American–British subtypes, which is in agreement with the findings of previous studies.[15,16] *CEBPA* mutations were predominant in the intermediate risk and normal karyotype group, which is also consistent with previous findings.[15–17]

With regard to prognosis, the results presented herein suggest that *CEBPA* mutations, especially *CEBPA*-double, are an independent favorable prognostic factor in pediatric AML patients. Multivariate analysis of the normal karyotype cohort identified *CEBPA*-double as an independent favorable prognostic factor for EFS, but not OS; this finding may be due to the small sample size. As the majority of pediatric AML patients lack markers that indicate a favorable or poor prognosis, it is important to identify prognostic markers in intermediate-risk patients. *CEBPA* mutations show promise as markers of a favorable prognosis in pediatric AML patients, because they are strongly associated with intermediate risk.

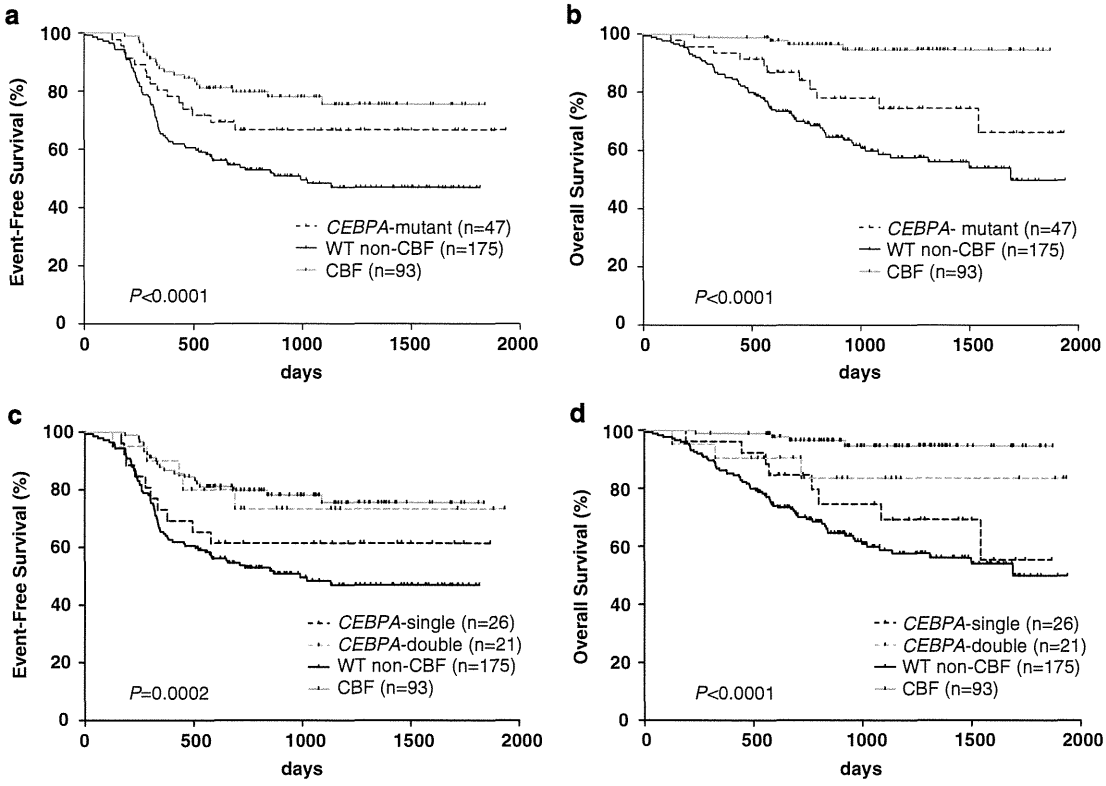

Figure 2. Kaplan–Meier survival curves showing EFS and OS from the time of diagnosis according to *CEBPA* mutation status. (**a**) EFS and (**b**) OS of patients harboring *CEBPA* mutations, patients harboring WT *CEBPA* (excluding core-binding factor-acute myeloid leukemia (CBF-AML) cases (WT non-CBF)) and patients with CBF-AML. (**c**) EFS and (**d**) OS of patients harboring a single *CEBPA* mutation (*CEBPA*-single), patients harboring double or triple *CEBPA* mutations (*CEBPA*-double), WT patients (excluding CBF-AML cases (WT non-CBF)) and patients with CBF-AML. *P*-values were determined using the log-rank test.

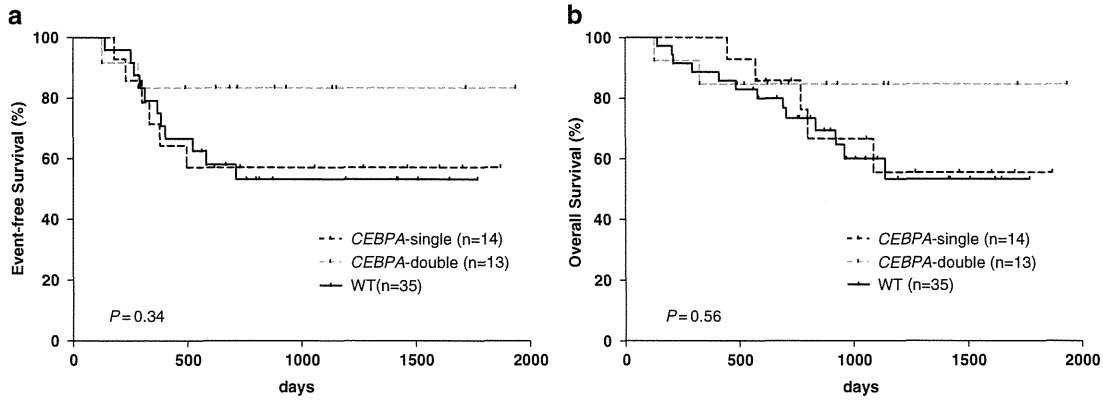

Figure 3. Kaplan–Meier survival curves showing EFS and OS in acute myeloid leukemia patients with a normal karyotype. (**a**) EFS and (**b**) OS of patients harboring a single *CEBPA* mutation (*CEBPA*-single), patients harboring double or triple *CEBPA* mutations (*CEBPA*-double) and WT patients. *P*-values were determined using the log-rank test.

Consistent with our results, several studies (including one pediatric study) postulated that AML patients harboring double *CEBPA* mutations have a favorable prognosis.[9–12] Two different *CEBPA* mutations have a synergistic effect on AML development, and the mechanism underlying leukemogenesis is likely to be different from that in AML patients harboring a single *CEBPA* mutation.[24,25] We found that a combination of N-terminal and C-terminal mutations is essential for a better prognosis in *CEBPA*-double patients (data not shown), indicating that a favorable prognosis is restricted in patients who lack WT CEBPA p42 expression among *CEBPA*-double patients. Moreover, a recent study of a large cohort of adult AML patients suggests that patients harboring double *CEBPA* mutations belong to a genetically distinct subtype and should be clearly distinguished from patients harboring a single mutation.[13] In this study, we could not examine the prognostic impact of concomitant molecular mutations because of their low incidence; therefore further analyses of pediatric AML patients is required.

In contrast to double *CEBPA* mutations, the prognostic value of single *CEBPA* mutation is currently under debate because of its small number. We detected a relatively large number of cases harboring a single *CEBPA* mutation in the total cohort, and

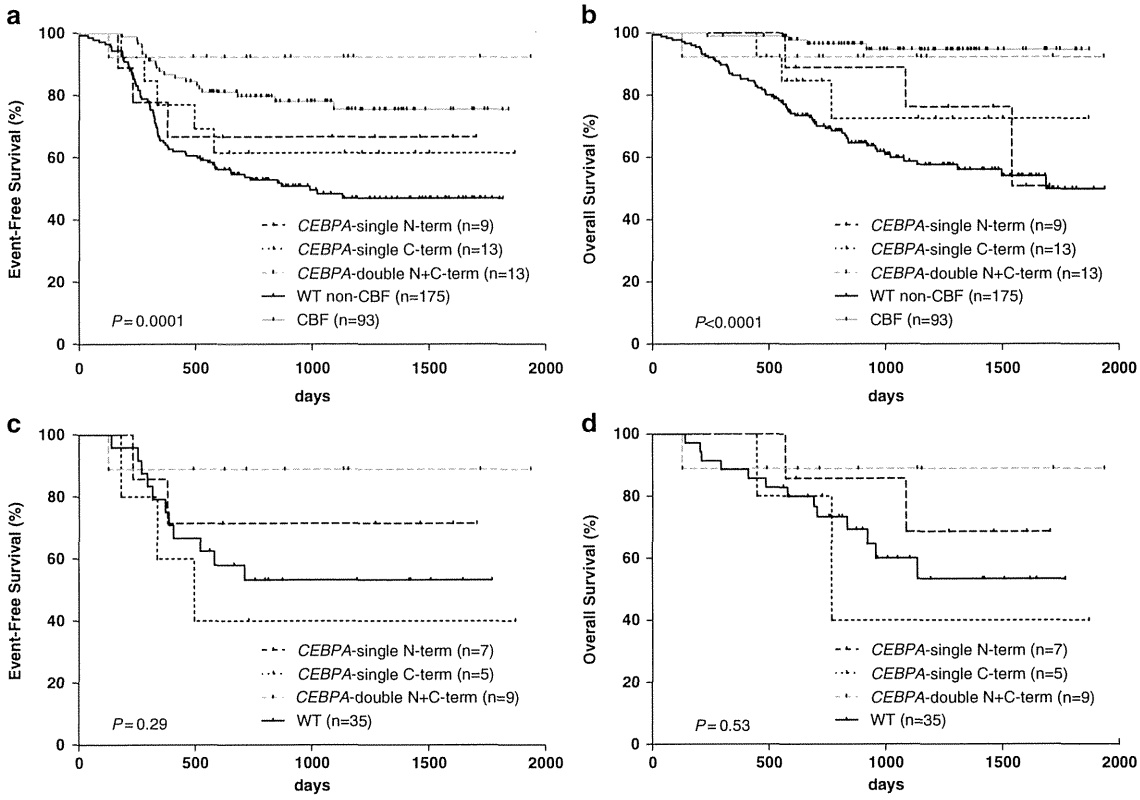

Figure 4. Kaplan–Meier survival curves showing EFS and OS according to the location and number of *CEBPA* mutations. Only patients with hotspot mutations predicted to cause p30 isoform translation and/or disruption or loss of the C-terminal bZIP domain were included in the analysis. (**a**) EFS and (**b**) OS in patients harboring a single N-terminal mutation (*CEBPA*-single N-term), patients harboring a single C-terminal mutation (*CEBPA*-single C-term), patients harboring both N and C-terminal mutations (*CEBPA*-double N + C-term), WT patients (excluding core-binding factor-acute myeloid leukemia (CBF-AML) cases (WT non-CBF)) and patients with CBF-AML. (**c**) EFS and (**d**) OS of AML patients with a normal karyotype. *P*-values were determined using the log-rank test.

Table 3. Multivariate Cox regression analysis for EFS and OS

	EFS			*OS*		
	HR	*95% CI*	P-*value*	*HR*	*95% CI*	P-*value*
Total cohort (n = *315*)						
Mutation status, vs WT non-CBF						
CBF	0.31	0.19–0.49	<0.01	0.09	0.03–0.25	<0.01
CEBPA-single	0.47	0.24–0.91	0.02	0.60	0.29–1.26	0.18
CEBPA-double	0.33	0.14–0.76	0.01	0.30	0.09–0.94	0.04
Age (+1 year)	1.00	0.97–1.03	0.86	1.03	0.99–1.07	0.17
WBC (⩾50 000)	1.81	1.29–2.55	<0.01	1.50	0.96–2.33	0.07
Normal karyotype cohort (n = *62*)						
Mutation status, vs WT						
CEBPA-single	0.54	0.22–1.33	0.18	0.88	0.31–2.47	0.81
CEBPA-double	0.28	0.08–0.95	0.04	0.49	0.11–2.17	0.35
Age (+1 year)	0.95	0.89–1.02	0.14	0.94	0.86–1.02	0.13
WBC (⩾50 000)	2.05	1.00–4.22	0.05	1.34	0.55–3.29	0.52

Abbreviations: CBF, core-binding factor; *CEBPA*, CCAAT/enhancer-binding protein alpha; CI, confidence interval; EFS, event-free survival; HR, hazard ratio; OS, overall survival; WBC, white blood cell count; WT, wild type.

multivariate analysis identified single mutation as an independent prognostic factor for favorable EFS (Table 3). Two adult AML studies (but no pediatric studies) showed that a single *CEBPA* mutation can be an independent favorable prognostic factor in patients harboring *NPM1* mutations.[26,27] Indeed, the two patients in the present study that harbored both a single *CEBPA* mutation and an *NPM1* mutation showed good long-term survival without any events. We also tried to examine the clinical significance of the location of the mutation in *CEBPA*-single patients but found no significant difference in outcomes for patients harboring N-terminal or C-terminal mutations. However, the *CEBPA*-single patients in the normal karyotype cohort who harbored a